Persistence and plasticity in conifer water-use strategies

M. Berkelhammer[1], C. Still[2,3], F. Ritter[1], M. Winnick[4,5], L. Anderson[6], R. Carroll[7], M. Carbone[8], & K. Williams[2,9]

[1]Dept. of Earth and Environmental Sciences, University of Illinois at Chicago
[2]Rocky Mountain Biological Laboratory, Gothic, CO
[3]Dept. of Forest Ecosystems and Society, Oregon State University
[4]Dept. of Geological Sciences, Stanford University
[5]Dept. of Geosciences, University of Massachusetts Amherst
[6]United States Geological Survey, Geosciences and Environmental Change Science Center, Denver, CO
[7]Division of Hydrological Sciences, Desert Research Institute, Reno, NV
[8]Dept. of Biological Sciences, Center for Ecosystem Science and Society, Northern Arizona University
[9]Lawrence Berkeley National Laboratory, Department of Energy

Key Points:

- Cellulose isotope ratios were used to reconstruct the use of snowmelt for two common conifer species in the southern Rocky Mountains.
- The trees exhibited multi-year periods of preferential use of snowmelt and low tree growth following low snowpack years.
- During high snowpack periods the trees showed enhanced growth and utilized summer precipitation to support their increased water demands.

Corresponding author: M. Berkelhammer, berkelha@uic.edu

Abstract

The selective use of seasonal precipitation by vegetation is critical to understanding the residence times and flow paths in watersheds, yet there are limited datasets to test how climate alters these dynamics. Here, we use measurements of the seasonal cycle of tree ring $\delta^{18}O$ for two widespread conifer species in the Rocky Mountains of North America to provide a multi-decadal depiction of the seasonal origins of forest water use. The results show that while the conifer tree stands had a dominant preference for use of snowmelt, there were multi-annual periods over the last 4 decades when use of summer precipitation was preferential. Utilization of summer rain emerged during years with increased snowfall and tree growth, suggesting that summer rain enhanced the transpiration stream only during the periods of highest water use. We hypothesize this could be explained through shallowing of the root profile during wetter periods and/or through the effects of the water table depth on the residence time of summer precipitation in the root zone. We suggest the tree ring proxy approach used here could be applied in other watersheds to provide critical insight into the temporal dynamics of plant water use that could not be inferred from short measurement campaigns. These data on the seasonal origins of forest water are critical for understanding forest vulnerability to drought, the processes that affect precipitation pathways and residence time in watersheds and the interpretation of tree ring proxy data.

1 Introduction

Ecosystems often display multi-annual legacy effects as illustrated by the fact that tree ring widths tend to display lower frequency variability than limiting factors for productivity such as precipitation or temperature (Bunde, Büntgen, Ludescher, Luterbacher, & Von Storch, 2013; Esper, Schneider, Smerdon, Schöne, & Büntgen, 2015). One interpretation of this low frequency behavior is that it reflects biotic processes such as the use of a previous year's non-structural carbon pool or changes in leaf area that affect photosynthesis for subsequent seasons (Bréda, Huc, Granier, & Dreyer, 2006; Franke, Frank, Raible, Esper, & Brönnimann, 2013; Sala, Gherardi, Reichmann, Jobbagy, & Peters, 2012). However, year-to-year persistence in aboveground productivity may also emerge abiotically through the dynamics of subsurface hydrology such as the lagged and sustained response of water table depths or deep soil moisture content to precipitation variability (Amenu, Kumar, & Liang, 2005; Bierkens & Van den Hurk, 2007; Kumar, Newman, Wang, & Livneh, 2019; Maxwell & Kollet, 2008). It follows, if plants are relying on deeper soil moisture or water pools held in low matric potential pores with long residence times, then multi-annual persistence in ecosystem productivity could emerge through the delayed and sustained response of soil hydrology to surface climate (Ghannam et al., 2016; Rempe & Dietrich, 2018). A number of studies using water isotopic tracers (Dawson & Pate, 1996; Zhang, Evaristo, Li, Si, & McDonnell, 2017) and root excavations (Fan, Miguez-Macho, Jobbágy, Jackson, & Otero-Casal, 2017) have observed that maximum rooting depths often track the water table depth suggesting plants actively subsidize their water demands with older and deeper water pools. These observations support modeling results, which indicate that in order to accurately capture spatial patterns in transpiration and the response of terrestrial ecosystems to precipitation variability, it is imperative to account for precipitation from previous seasons or years (Ferguson, Jefferson, Maxwell, & Kollet, 2016; Maxwell & Condon, 2016; Maxwell, Condon, Danesh-Yazdi, & Bearup, 2019).

Although the ability for plants to utilize deeper water pools is a widespread adaptation, the extent to which plants actively rely on these legacy water reservoirs is difficult to constrain. Some studies have suggested that trees can switch between use of deep and shallow water reservoirs depending on water availability (Dawson & Pate, 1996), while other studies have shown that species consistently rely on deeper water to minimize competition (Anderegg, Anderegg, Abatzoglou, Hausladen, & Berry, 2013; Nardini et al., 2016). Attempts to understand the dynamics of this behavior have periodically taken advantage of precipitation exclusion experiments to force surface soil moisture deficits (Romero-Saltos, Sternberg, Moreira, & Nepstad, 2005), which have shown that root water uptake can have a threshold-like response to drying of surface soil moisture (Grossiord et al., 2017). The available observations suggest the wa-

ter use behaviors of trees can be diverse between sites and species, which likely reflects the interplay between subsurface hydrological characteristics, species competition, physical properties of the soil, physical and nutrient limitations on root growth, and the availability of carbon pools to invest in root development.

Much of the existing work on understanding plant water use has relied on the use of stable water isotopes (δ^{18}O and δ^{2}H) to trace the depth and seasonal origins of water uptake. A rigorous assessment of the isotopic ratio of soil water in the Shale Hills Critical Zone Observatory by Thomas et al. (2013) showed that surface soil water had an isotopic ratio that closely followed recent precipitation and the seasonal signal attenuated and approached groundwater values with increasing depth. In regions such as the western US where recharge occurs from winter snowpack, a strong isotopic gradient emerges during the growing season because the surface and deep soil waters originate from summer and winter season precipitation, respectively (Hu, Moore, Burns, & Monson, 2010; Martin, Looker, Hoylman, Jencso, & Hu, 2018). However, the idealized case where isotopically enriched summer precipitation is layered atop isotopically depleted winter precipitation is often disrupted by processes such as rapid penetration of rain through preferential flow paths, hydraulic redistribution, lateral flow and waters of distinct seasonal origins being held selectively according to pore size (Berry et al., 2018; Brooks, Barnard, Coulombe, & McDonnell, 2010; Dubbert & Werner, 2019; Sprenger, Llorens, Cayuela, Gallart, & Latron, 2019; Thomas et al., 2013). Furthermore, the presumably simple transfer of the isotopic ratio of precipitation to the surface soil water can be affected by evaporative enrichment of the surface water and precipitation throughflow effects as precipitation interacts with the canopy (Goldsmith et al., 2019).

These aforementioned studies capture a small cross section of new works that have collectively challenged the idea of using stable water isotopes in the xylem as a simple tracer for depth of water uptake (Sprenger, Leistert, Gimbel, & Weiler, 2016). Despite this evidence of complexity in depth and spatial pattern of soil water isotopes, other recent work has found more homogenous patterns in the isotopic ratio of plant water, suggesting some of the isotopic heterogeneity observable within soil water profiles might be buffered as the signal is transferred to plants (Goldsmith et al., 2019). The extensive survey of xylem waters across Switzerland by Allen, Kirchner, Braun, Siegwolf, and Goldsmith (2019), noted that across a large domain the trees appeared to rely almost exclusively on winter precipitation. This observation could reflect multiple interacting processes including: the ubiquitous reliance of trees on deeper water pools; deeper water from a previous season migrating upward into the root zone; winter precipitation being retained in micropores; or that summer precipitation evaporated or passed through the root zone in macropores. Nonetheless, the common use of winter precipitation by trees strongly supports the role of soil hydrology in adding a seasonal or even interannual legacy component to ecosystems (Kumar et al., 2019).

The existing studies on plant water use have generally taken advantage of spatial surveys or intensive studies over the course of a few growing seasons to infer the patterns of plant water use. There are limited data to test how these dynamics might evolve over longer timescales in response to stressors such as decreases in spring snowpack or rising evaporative demand (Mote, Li, Lettenmaier, Xiao, & Engel, 2018; Restaino, Peterson, & Littell, 2016). For example, existing data on water use by conifers in the western US have indicated that snowmelt, the predominant source of regional recharge, is the primary reservoir to support forest water demand (Bowling, Schulze, & Hall, 2017; Hu et al., 2010; Marshall & Monserud, 2006; Martin et al., 2018; Phillips & Ehleringer, 1995). However, the snapshots provided by these studies do not indicate how reliance on this water source has varied in response to region-wide changes in the snowpack or lengthening of the growing season. In one scenario, plants might conserve their total water use by modifying their water source, such as increasing use of summer rain. We refer to this as water-use *plasticity* where through either adjustments in the root systems or changes in the residence time and pathway of seasonal precipitation vectors, the seasonal origins of the water used by the trees evolves. In an alternative scenario, trees conserve their reliance on winter precipitation, which we refer to as the *persistence* scenario, and seems to be consistent with the ubiquitous use of winter precipitation as described by Allen et al. (2019). To study these dynamics, decadal length datasets of plant water use are needed

because many of the relevant subsurface processes such as residence time of deep water pools (Ghannam et al., 2016) and the turnover time of fine roots (Matamala, Gonzalez-Meler, Jastrow, Norby, & Schlesinger, 2003) have multi-annual timescales. Therefore, the ecohydrological response time and/or adjustment to change may lag the forcing and persist for years after the stressor has been removed.

One approach to studying longer term dynamics in plant water use is through measurements of δ^{18}O cellulose. Tree ring δ^{18}O captures a mixed signal of the vapor pressure deficit (VPD) at the leaf-atmosphere interface and the δ^{18}O of the plant's source water (Burk & Stuiver, 1981; Gessler et al., 2014; Roden, Lin, & Ehleringer, 2000). Higher VPD (or lower RH) acts to enrich the isotopic ratio of the leaf water and cellulose whereas changes in the source water have a proportionate influence on the cellulose. In conditions where the source water is constant, timeseries' of cellulose δ^{18}O can provide a robust proxy for VPD (Kahmen et al., 2011). Alternatively, if VPD is held constant, such as for aquatic plants (DeNiro & Epstein, 1981), the isotopic ratio of cellulose is a proxy for the isotopic ratio of the source water. In most terrestrial ecosystems, both of these variables change over time and the signal embedded in the cellulose is convolved. To address this, an estimate of one or the other variable (i.e. VPD or source water) is needed. In instances where an annual or multi-annual average of δ^{18}O is used, it is often assumed that the relative variability of VPD is larger than δ^{18}O of source water. Therefore, changes in the isotopic ratio of signal are more strongly affected by canopy conditions than plant water use (Helliker et al., 2018). However, when annual growth rings are subsampled to produce seasonal cycles in δ^{18}O, changes in the source water over the growing season may be large enough to supersede the effects of changing VPD. In the western US, for example, the isotopic ratio of precipitation may vary by as much as 15‰ through the year (Buenning, Stott, Yoshimura, & Berkelhammer, 2012) and thus shifting use of winter or summer precipitation would impart an isotopic difference between cellulose formed early and late in the growing season. Treydte et al. (2014), for example, found that seasonal trends in tree-ring δ^{18}O predominantly mirrored trends in the source water, including recent precipitation and soil water pools, while short term variations from needle-water ^{18}O enrichment had much less of an effect.

In the following study, we use stable isotopic measurements of tree-ring cellulose to look at 4 decades of plant water use for two dominant conifer species (*Abies lasiocarpa* and *Picea engelmannii*) in the Rocky Mountains of Colorado, USA. The study was motivated by the question of how recent declines in spring snowpack have modified the water use patterns of forests in the region. To accomplish this, we analyzed the seasonal cycle of cellulosic δ^{18}O at two nearby forest stands sites in Colorado, USA. We then used a clustering analysis to organize the seasonal cycles based on their shape and a mechanistic model to classify the shape of the seasonal cycle into the type of water use pattern used by the tree during that growing season. After classifying the water use pattern for each of the last 40 years, we analyzed how tree water use has varied in response to snowpack variations. We found that while snowmelt was the primary water source for these trees, summer rain emerged as a critical water source during the periods of highest snowpack. This suggests that selective uptake or outflow of summer precipitation through watersheds will depend on the snowmelt inputs from the previous years. Although there are challenges to inferring plant water use from cellulose, the results show how this technique could be useful for understanding plant water use dynamics even in minimally instrumented watersheds.

2 Methods

2.1 Sampling of water isotope reservoirs

During the 2016 growing season, comprehensive isotope sampling was conducted in a mixed stand of trees (*Abies lasiocarpa*, *Picea engelmannii* and *Populus tremuloides*) along Copper Creek in Gothic, CO (38.9592°N, longitude: 106.9898°W and elevation: 2880 m) (Fig. 1). During the field season, approximately weekly sampling of soils and stems was done within or nearby the tree stand. Living stems were cut from the tree, the material near the leaves was

removed and the remaining sample was debarked. Soils were generally dug from two depths (0-10 cm and 10-20 cm) and periodically deeper soils were sampled using a bucket auger. Stem and soil samples were bagged and frozen shortly after collection. Water was extracted from both soil and xylem using a batch extraction method where samples were sealed in a glass tube and placed between two bored-out aluminum blocks (Vendramini & Sternberg, 2007). One of the blocks was heated, which drove water off the sample, and the other side was cooled to condense the moisture. The method was modified for field deployment in the following ways: (1) instead of a liquid nitrogen cold trap, we used a peltier cold plate kept close to -10°C, (2) a pair of 1" glass tubes with threaded ends enclosed the sample using a teflon union, which removed the need to seal the samples with a torch and allowed the tubes to be cleaned and reused and (3) after samples were sealed, vacuum was applied through a ball valve threaded into the union. The system was left overnight in this configuration to ensure all water was driven off the samples. Tests where soil was vacuum dried and then re-wet with a known quantity of water were used to ensure that this method produced greater than 95% water yield.

To mitigate the effects of hydrocarbon contaminants on the isotope spectroscopy, activated charcoal was added to the extracted water, which was covered with Parafilm and left for multiple hours. Following this, the samples were filtered to remove any particulates and then passed through a Solid Phase Extraction membrane to remove additional volatile compounds (Chang, Wolf, Gerlein-Safdi, & Caylor, 2016). Water samples were then analyzed on a Picarro Inc. L2130-i isotopic analyzer using an autosampler and vaporizer, which was maintained at 110°C. Samples were analyzed 8 times and ChemCorrect software was used to remove any spectral interferences. Following this, a memory correction (in the form of a double exponential fit) was applied to remove the influence of the previous sample and the final three injections from each sample were then averaged and normalized to the VSMOW scale using three in-house standards that were run prior to and during each run. We ran numerous tests of the system by vacuum drying soils from the site and rewetting them with a water of a known isotopic value. We determined an uncertainty of ~0.5‰ in δ^{18}O based on repeat analysis of the soil extraction system. An additional analysis was conducted where 26 soil samples were collected from a small grid nearby the field site. This was done to assess how both micro-scale hydrology affects the soil water isotopic ratios and the repeatability of the measurements considering sample handling, extraction and isotopic analysis (Johnson et al., 2017). The standard deviation of these samples was 1.1‰, which is similar though slightly smaller than the value of 1.7‰ found in a similar experiment by Goldsmith et al. (2019). We use this value as the presumed uncertainty of the soil water isotopic measurements.

To quantify the effect of alcohols and other volatile compounds on the xylem water samples, duplicate analysis on a subset of samples was done on both the laser system and with an isotope ratio mass spectrometry (IRMS). These samples were pyrolyzed at 1400°C in a ThermoFisher TC/EA and the resulting CO was introduced into a ThermoFisher Delta Plus IRMS through a Conflo II interface. Samples were calibrated using two in-house water standards. There was no systematic bias between the samples measured by the laser and the IRMS techniques. The observed differences were, on average, smaller than the repeatability uncertainty (i.e. extraction, processing and isotopic analysis). We take a conservative approach by averaging multiple samples to generate aggregated estimates of isotopic ratios and focus discussion only on high amplitude signals (i.e. ≥1.1 ‰ in δ^{18}O). Because isotopic analysis on the IRMS was done for δ^{18}O, we hereafter only discuss variability in terms of oxygen isotopes.

Weekly precipitation samples were obtained from the following nearby US Department of Agriculture, National Atmospheric Deposition Program (NADP) sites: Gothic, CO (NADP ID: CO10, latitude: 38.956°N, longitude: -106.986°W, elevation: 2915 m), Sunlight Peak (NADP ID: CO92, latitude: 39.4264°N, longitude: -107.3799°W, elevation: 3218 m) and Four Mile Park (NADP ID: CO08, latitude: 39.4025°N, longitude: -107.3454°W, elevation: 2502 m) (Fig. 1 and Table S2). Samples from Gothic were obtained for the 2016 growing season whereas data from the other sites extended from 2007 to 2017 (Table S2). The accumulated annual April 1 snowpack from 1993 through 2016 at Sunlight Peak, CO and Four Mile Park, CO were extracted from the Anderson, Berkelhammer, and Mast (2016) database. Weekly stream water samples were collected from Copper Creek, which flows near the tree stand and groundwa-

ter was collected from regularly sampled from three wells in Gothic, CO. The isotopic ratio of snowpack, groundwater and precipitation were all determined using the same Picarro Inc. analyzer as used for the xylem and soil water samples. Water vapor isotopic ratios were measured continuously and binned to a 30-minute resolution from an inlet installed on a 10 m tower at the EPA instrument trailer in Gothic, CO during May and June of 2016. Details of the approach to continuously measure the isotopic ratio of water vapor have been described elsewhere (Berkelhammer et al., 2016). The aggregated isotopic data discussed above was utilized in two ways. Firstly, we used the xylem and soil water isotopes for 2016 to develop direct observational constraints on the reliance of winter and summer precipitation by the trees over the course of a single growing season. Secondly, we used the longer precipitation, snowpack and vapor samples as inputs to a mechanistic model (as described in Section 2.4) to understand how changing water use patterns would influence the seasonal cycle of the isotopic ratio of cellulose.

2.2 Measurements of isotopic ratio of cellulose

During 2015 and 2016, 19 tree cores were collected using a 5 mm increment borer from stands near Copper Creek in Gothic, CO and nearby the Ziegler Reservoir in Snowmass, CO (39.2075°N, 106.9648°W) (Brown, Nash, & Kline, 2014) (Fig. 1). Cores were taken at each site from 4-5 mature *A. lasiocarpa* and *P. engelmannii* trees that were selected based on having similar diameters, occurring away from the edge of the stand and a healthy appearance. Cores were sanded, scanned, rings counted and widths measured using an image-processing script. Width chronologies were standardized by removing the geometric effect of increasing stem circumference using a low frequency filter. The resulting ring widths were normalized and all cores averaged to produce a composite ring width chronology. From the 19 tree cores collected and used for the ring width measurements, 9 were chosen for isotopic analysis based on having the highest correlation coefficient with the composite ring width chronology. This subsetting from the full collection was done to minimize analytical costs of isotopic analysis while still providing a large population of data for subsequent analysis. Tree cores were sliced starting from the most recent rings and working towards the inner ring (Fig. 2). Individual slices were combined until 1.0 to 1.2 mg of sample was accumulated, which was the minimum size that would allow sufficient material for isotopic analysis following cellulose extraction. Of the ~330 rings associated with the 9 tree cores from 1980-2016, 135 yielded a sufficient number of samples to be included in the analysis (≥5 per ring) (Schubert & Jahren, 2015). A regression between the number of rings per year and ring width show that the analysis was not weighted towards use of years with wide rings (Fig. S1). Each wood sample was then powdered and the cellulose extracted from the whole wood using the Brendel method (Anchukaitis et al., 2008; Berkelhammer & Stott, 2012). Briefly, samples were heated in a mixture of acetic and nitric acid to remove non-cellulosic material and then subjected to subsequent washes with ethanol, deionized water and acetone. Samples were then dried for 1 hour in a drying oven, left overnight in a vacuum oven and stored in a desiccator. The cellulose yield was generally between 40-60% of the initial wood mass.

Isotopic analysis of the cellulose was conducted at Northwestern University, Northern Illinois University and University of Illinois at Chicago stable isotope labs following similar procedures. Between 0.2 and 0.5 mg of cellulose was weighed into a silver capsule and loaded into a Costech Zero Blank autosampler. The samples were then pyrolyzed at ~1350°C in a TC/EA using a ceramic column with an interior glassy carbon liner. The isotopic ratio of the resulting CO gas (i.e. $^{12}C^{18}O/^{12}C^{16}O$) was then analyzed on a ThermoFisher Delta series IRMS. A typical run would begin with analysis of three replicates of one organic reference standard (such as cellulose or sucrose), three replicate analysis of a second reference standard followed by sequential analyses of 8 samples and a single reference standard. The run would then terminate with duplicate analyses of each of the reference standards. A sample carousel with 49 slots would thus typically include 36 samples and 13 standards, which were used for drift correction and normalization to the VSMOW-scale. Duplicate analyses of reference standards showed an analytical uncertainty of ≤0.2‰.

2.3 Processing of the isotopic measurements

The shape of the isotopic cycle in the annual growth ring reflects a combination of seasonal changes in leaf-atmosphere exchange, the trees' source water, and internal mixing of water and carbohydrates that generate lags and buffering effects (Ogée et al., 2009). Our *a priori* assumption was that if a tree relied exclusively on winter precipitation through the growing season, this would generate a distinct isotopic cycle in the cellulose than if the tree relied on a seasonally evolving summer precipitation source. We can then extend the analysis of tree water use from the single season we monitored (i.e. 2016) by analyzing how the shape of the seasonal cycle in cellulose δ^{18}O has changed over time. To achieve this, we interpolated all annual cycles to a common resolution of 7 samples/year following the approach of Schubert and Jahren (2015). The mean of all values from each growth ring was then subtracted to generate a seasonal cycle of isotopic anomalies. We used anomaly values instead of absolute isotopic ratio to facilitate comparison between seasonal cycles of years with different mean isotopic ratios. After generating these seasonal cycles for all available years, we aggregated all data from the two species (*A. lasiocarpa* and *P. engelmannii*) and two sites (Gothic, CO and Ziegler Reservoir) as part of a single population that included all 135 cycles over the period from 1980-2016. The decision to aggregate data provided a larger population of data for subsequent analyses and was justified based on the observation that the seasonal isotopic cycle and absolute isotopic values between species and sites were not statistically different (Fig. 3). This suggests that the trees at these nearby sites utilize similar water reservoirs and experience similar canopy conditions though future work could benefit from considering how small differences between species might reflect species-specific ecophysiology or ecohydrology.

To characterize the dominant isotopic cycles, a k-means clustering algorithm was utilized on the full population of seasonal cycles. The purpose of the clustering algorithm was to take the full population of seasonal isotopic cycles and partition them into a fixed number of groups (i.e. clusters) in a way that minimizes the difference between the cycles within a cluster and maximizes the difference between clusters. This is done using an iterative approach where isotopic cycles are sorted randomly into a fixed number of clusters, the centroid (or average of the cluster) is calculated and the average difference between each member of the cluster and the centroid is calculated. This process is repeated until the sorting produces the smallest accumulated difference between the members of each cluster and the mean of the cluster. Here, we used the Pearson's correlation coefficient to calculate the difference between each member of a cluster and the centroid and we ran the algorithm for 10,000 iterations. A critical aspect of using k-means clustering is the *a priori* decision of how many clusters to sort the data into. After experimenting with a range of cluster sizes from 2-8, we chose to sort the seasonal cycles of the isotopic ratio of cellulose into three clusters. This choice was governed by the fact that as we increased the number of clusters, the same three dominant clusters persistently emerged while the additional clusters contained only a small number of cycles. An example of this analysis is illustrated in Figures S2 and S3. Lastly, after categorizing each cycle into one of the three clusters, we generated a timeseries of the relative frequency of each of the clusters over the period from 1980-2016 to assess how tree water use has shifted over recent decades.

2.4 Modeling of isotopic ratio of cellulose

In order to provide a mechanistic understanding of the dominant patterns in tree cellulose δ^{18}O that emerged from the cluster analysis, we used a model for the isotopic ratio of cellulose to explore how changes in seasonal water use influenced the shape of the annual cycle in tree ring cellulose. The model is based on the following equation:

$$\delta^{18}O_{cellulose} = \delta^{18}O_{source} + (1 - pe) * \Delta_{leaf} + \epsilon \quad (1)$$

Where the $\delta^{18}O_{cellulose}$ is modeled as a mixture between the isotopic ratio of the source water for the tree ($\delta^{18}O_{source}$) and the isotopic ratio of the leaf water (Δ_{leaf}) that has been

enriched by transpiration relative to $\delta^{18}O_{source}$. The photosynthates that form in the presence of the leaf water are further enriched in ^{18}O by a biochemical fractionation factor (ϵ, Equation S10). The relative importance of the source water and leaf water in defining the isotopic ratio of the cellulose is set by a mixing term defined as *pe*. The mixing term ranges from 0-1 and describes the efficiency with which isotopic exchange between photosynthates and xylem water occurs during cellulose metabolism. This model and close variants have been used in numerous studies and we refer readers to Barbour, Roden, Farquhar, and Ehleringer (2004); Evans (2007); Keel et al. (2016); Ogée et al. (2009); Roden et al. (2000) and references therein for additional details.

Detailed information on the isotopic ratio of xylem, soil, precipitation and groundwater were available from our 2016 field season, which provided a single season's constraint on $\delta^{18}O_{source}$. To estimate the source water over the full period when cellulose data was available (i.e. 1980-2016), we took advantage of the 20 years of the isotopic ratio of April 1 snowpack from Anderson et al. (2016) to provide a constraint on the winter precipitation and 10 years of weekly precipitation samples from nearby NADP sites to provide estimates of the summer rain input (Figs. 4 and 5). Both the snowmelt and summer precipitation inputs were estimated back to 1980 by calculating the climatological average from all available data and using this value for years when observations were not available. Using these summer and winter precipitation inputs, we tested how the relative utilization of these two water sources over this time period influenced the seasonal cycle of cellulose.

To estimate the other key term in Equation 1, Δ_{leaf}, we needed estimates of the physiological and canopy terms that influence isotopic exchange between leaf water and the atmosphere (e.g. transpiration, leaf VPD and canopy conductance). In the absence of direct canopy measurements, we inferred the canopy terms using the canopy model Soil Canopy Observation Photosynthesis Energy Model (SCOPE) (van der Tol, Verhoef, Timmermans, Verhoef, & Su, 2009; van der Tol, Berry, Campbell, & Rascher, 2014). SCOPE is a 1-D vertical model (40 canopy layers) that solves for the canopy energy budget, thermal properties of the canopy, radiative transfer of fluorescence, sensible and latent heat fluxes, resistance terms (from wind speed and canopy properties) and stomatal conductance and photosynthesis using the Farquhar-Berry model, which assumes photosynthesis is limited by light (electron transport) or Rubisco carboxylation and stomatal conductance, which together influence chloroplast CO_2 concentration (van der Tol et al., 2014). While this model lacks key ecosystem dynamics that are present in land surface models (such as the stomatal response to changing soil moisture), it is an efficient tool to estimate how canopy conditions respond to radiation, temperature and humidity changes. The model was run with a 30-minute time step from 1980-2016 using the following inputs mostly extracted from the North American Regional Reanalysis (NARR), which has a temporal resolution of 3 hours and spatial resolution of 32 km (Mesinger et al., 2006): incoming longwave and shortwave radiation, barometric pressure, relative humidity, windspeed, atmospheric CO_2, canopy height and leaf area index (Table S1 and S4, Figs. S4 and S5). The climate forcing data from NARR was validated through a comparison with relative humidity and air temperature data from three nearby meteorological stations, referred to as billy barr (sic), Snodgrass and Mexican Cut (Figs. S6 and S7). We used the meteorological data to provide estimates of systematic bias and random uncertainty in the meteorological forcing that emerge from errors in NARR and the presence of subgrid cell variability in this topographically complex region. However, since these meteorological stations are neither maintained nor calibrated to National Weather Service standards, they are only used here to provide a point of comparison to assess model errors. The NARR data was interpolated from 3-hourly to 30-minute resolution, which was the timestep required to close the energy balance in the SCOPE simulations. Atmospheric CO_2 data was downloaded from the NOAA GMD flask measurements from Niwot Ridge. The Leaf Area Index and canopy height were set at fixed values of 3.0 m^2 m^{-2} and 10 m, respectively, based on estimates from satellite retrievals in Liang et al. (2013) and Simard, Pinto, Fisher, and Baccini (2011).

To solve for Δ_{leaf} in Equation 1, the modeled estimates of transpiration, photosynthesis, leaf temperature, leaf VPD and canopy conductances from SCOPE were passed through Supplementary Equations 1-10 (Barbour et al., 2004; Keel et al., 2016; Ogée et al., 2009; Ro-

den et al., 2000). The cellulose model also required estimates of the path length of the leaf, which was set at a fixed value of 0.01 cm (Keel et al., 2016), and the exchange efficiency between xylem water and sugars during cellulose metabolism (i.e. *pe*), which was set at 0.42 (Roden et al., 2000). The model produced 30-minute estimates of the isotopic ratio of cellulose for all time-steps when photosynthesis was greater than 0 and the air temperature was above the critical threshold for xylogenesis (Rossi et al., 2008). To convert the model results into annual cycles for the isotope ratio of cellulose with comparable resolution as the observations, we took the total accumulated photosynthesis for the growing season and distributed it into 7 equal segments and then calculated weighted averages of δ^{18}O of cellulose (weighted by rate of photosynthesis) for each of the 7 segments. A visual depiction of the full modeling framework is shown in Figure 6.

The model described above was utilized here in two ways:

(1) To simulate seasonal cycles of δ^{18}O for each year from 1980-2016 with the same atmospheric forcing but with three different water use patterns; only winter precipitation, only summer precipitation, or a transition between use of winter to summer precipitation midway through the growing season (Fig. 5). The outcome of this modeling exercise was 37 annual isotopic cycles (1980-2016) for each of the three water use patterns. This analysis tested both how interannual changes in atmospheric forcing affected the seasonal cycle in cellulose even if the water use was held constant and how the average seasonal cycle would change if the water use pattern was altered.

(2) To simulate a single year (2016) with the three different water use scenarios while the following input parameters were varied using a Monte Carlo simulation: canopy temperature, δ^{18}O of the water vapor, δ^{18}O of the source water, relative humidity, transpiration, the exchange efficiency with xylem water during cellulose metabolism (i.e. *pe*) and the rate of photosynthesis. These terms were chosen for the Monte Carlo simulation because they have the largest impacts on the final estimates of the isotopic ratio of cellulose and are terms that are difficult to constrain. We altered each of these terms in two ways: (1) we added a uniformly distributed ±20% error to each 30 minute timestep and (2) we added ±20% bias to all the values of that term for the entire year. We then ran 10000 simulations producing a distribution of annual cycles in δ^{18}O for a single year for each of the three water use patterns. The goal of this exercise was to assess the extent to which random uncertainty or bias in the key terms of the cellulose model might influence the shape of the seasonal cycle.

3 Results

Through May and early June of 2016, the measured soil water was dominated by snowmelt and the isotopic ratio of the soil water was homogenous with depth and similar to both the isotopic ratio of groundwater and April 1 snowpack (-18‰±0.5) (Fig. 4). During this period, the stable isotopic ratio of xylem waters from *A. lasiocarpa* and *P. engelmannii* were comparable to the depth-averaged soil water (Fig. 4). As the growing season progressed, the isotopic ratio of the xylem water was invariant while precipitation increased to ~-10‰ and surface soil water increased to ~-12‰. By July (day of year 180-200), it was evident from the low isotopic ratios in the xylem water that the trees remained reliant on winter precipitation and were likely drawing on a mixture of water that included sources at least 50 cm below the surface but could have been drawing on water as deep or deeper than 130 cm. Root excavations for *Abies* and *Picea* species elsewhere have found rooting depths of 240 cm and 160 cm, respectively (Fan et al., 2017), which are within the ranges suggested by the isotopic analysis presented at this site. Beginning late July (day of year 210), the isotopic ratio of the xylem waters began to increase, reaching isotopic ratios of ~-5‰ by mid-August. These values were comparable to surface soil water and precipitation at that time. The transition from use of winter to summer precipitation occurred weeks after a ~2 m drop in the water table height and a 50% decline in soil moisture at 50 cm, perhaps a response to transpiration uptake, but occurred nearly simultaneously with a modest increase in both 5 cm and 15 cm soil moisture levels (Fig. S8).

The 2016 data provide evidence for a water use pattern characterized by a transition between use of winter to summer precipitation midway through the growing season (Fig. 5). This behavior is consistent with observations of water use from previous studies in the region (e.g. Hu et al. (2010)) but is not of sufficient length to assess the long term persistence of this pattern. We thus utilized the cellulose δ^{18}O data to examine temporal variations in the water use pattern. The entire population of 780 cellulose δ^{18}O measurements span between 26 to 36‰, which encompasses the range found in other isotopic studies on conifers from the region (Belmecheri, Wright, Szejner, Morino, & Monson, 2018; Berkelhammer & Stott, 2012; Szejner et al., 2016) (Fig. 3). Since there was no significant difference in the isotopic range or shape of the average annual cycle between sites (Ziegler Reservoir and Gothic) and species (*A. lasiocarpa*, *P. engelmanni*), we infer that they are responding to a common atmospheric forcing and water use pattern (Fig. 3). The average cellulose cycle observed at these sites is characterized by isotopic anomalies of +0.5‰ early in the season that transition to isotopic anomalies of -0.5‰ by the end of the growing season. This pattern is similar to what has previously been observed in trees in Arizona by Belmecheri et al. (2018) and in eastern California by Berkelhammer and Stott (2009). After partitioning all available cycles into three clusters, we found that the most common cycle (referred to as Cluster 1) was similar in structure to the average cycle (i.e. Fig. 3) and this pattern accounted for 48% of all the observed cycles (Fig. 7a). The second most common cycle (referred to as Cluster 2), has a quasi-parabolic structure with isotopic anomalies of -1‰ in the beginning and end of the season and a mid season maximum of +1 ‰ (Fig. 7b). The years in this cluster accounted for 30% of all the observed cycles. The last cycle, referred to as Cluster 3, was similar in structure to Cluster 1 during the first half of the growth ring but then deviated by showing a progressive rise through the latter half of the growing season (Fig. 7c). The years that fell within this cluster accounted for 22% of the observed cycles. The growth rings and xylem water measurements from 2016 fell within the population included in Cluster 3 (Fig. S9).

To explore the processes that gave rise to the distinct clusters, we ran the cellulose model over the period from 1980-2016 with three distinct water use patterns: (1) exclusive reliance on snowmelt/winter precipitation as observed by Allen et al. (2019), (2) reliance on growing season precipitation (Belmecheri et al., 2018) and (3) the water use pattern observed from field observations during 2016, which was characterized by a mid season transition between reliance on winter to summer precipitation (Fig. 5). When the model was run with a winter precipitation water source, the average seasonal cycle over the 37 year simulation closely followed the structure of Cluster 1 (Figs. 7a and 7e). In contrast, when the model was forced with a summer precipitation source, the pattern mirrored Cluster 2 (Figs. 7b and 7f) and when the model was run with the water source pattern of 2016, the modeled structure followed Cluster 3 (Figs. 7c and 7g). When comparing the modeled and observed cellulose cycles, it is important to note that the tree ring measurements do not have a timestamp but rather a fractional position in the ring (Fig. 2). The similarity between modeled and observed cycles may allow us to place an absolute timestamp on when the cellulose layers were formed. However, this is contingent on the seasonal cycle in the model being accurate. We assessed this by comparing the modeled transpiration rate with sap flux from the Gothic tree stand (Fig. S10), which supports that the canopy conditions simulated by the model, were sufficient to reproduce the broad timing of when the trees were transpiring even though there was not sufficient information to quantitatively compare the absolute magnitude of the observed and modeled transpiration fluxes. An additional comparison was made between the modeled photosynthetic rate with satellite-derived gross primary production (GPP) from the monthly FluxSat product (Joiner et al., 2018), which is derived from a combination of MODIS reflectances, solar induced fluorescence retrievals and a light use efficiency model. This comparison suggested the SCOPE model had effectively captured the seasonal cycle in tree activity (Fig. S11). We did not attempt to quantitatively compare the modeled and satellite GPP because the resolution of the satellite product is 0.5° and the grid cell in which the trees fall includes a mixture of open forests (44%) and grasslands (55%). Lastly, we compared the modeled seasonal cycle in GPP with tree expansion from manual dendrometer bands at the Gothic site, which indicated these trees seemed to allocate a smaller fraction of late season GPP towards radial growth (Fig. 8). For

example, radial growth reached 90% of its annual total by day of year 200 (i.e. mid-July) while total carbon fixation did not reach 90% of its annual total until August. This apparent discrepancy can be explained by the fact that wood cells form and expand radially significantly ahead of when the cell walls thicken with cellulose. Thus, the temporal lag between volumetric growth and carbon allocated to cellulose observed here is consistent with data from the global analysis by Cuny et al. (2015) (Fig. 8). The result is also consistent with recent work on the isotopic composition of cellulose from other conifers in the southwestern US, which found that the isotopic ratio of cellulose within a tree-ring correlated most strongly with climate a month or more after the cells formed (Monson, Szejner, Belmecheri, Morino, & Wright, 2018; Szejner et al., 2016). Taken together, the comparison of the modeled transpiration and photosynthesis with sap flux, satellite GPP and dendrometry data all indicate that the modeled seasonal cycle in cellulose is approximately accurate.

The similarity between the δ^{18}O cycles that emerged from the three modeled water use scenarios and three dominant clusters derived from the observations (Fig. 7), suggests that changes in tree water use may explain the observed variations in the shape of the season cycles in cellulose δ^{18}O. However, because of uncertainty in some of the key forcing terms and parameters in the model, we remain cautious to limit interpretations of differences in the modeled seasonal cycles strictly in terms of changing water use. Notably, the most sensitive term in the cellulose model is relative humidity or leaf VPD (Burk & Stuiver, 1981; Kahmen et al., 2011) and our comparisons between RH from the local meteorological stations and the NARR grid cell show the potential for 10-20% errors in this forcing term (Fig. S6). The results from the Monte Carlo simulations indicate that the absolute δ^{18}O values are in fact highly sensitive to 20% model bias and error, such that the modeled seasonal cycles derived with the same water use can differ by 10‰ (Fig. 9, top row). However, when the absolute δ^{18}O are subtracted from the seasonal cycle and we consider isotopic cycles as anomalies relative to that year, the shape of the seasonal cycle is robust against model error and bias (Fig. 9, bottom row). This is an important distinction because it illustrates how modeling the absolute δ^{18}O value requires tight constraints on model parameters while modeling the shape of the seasonal cycle can be achieved despite high levels of uncertainty in model forcing terms. In light of these results, we focus discussion primarily on the observed seasonal patterns in the isotopic anomalies. Importantly, however, the distribution of modeled δ^{18}O values are not different than the population of observations, indicating that model forcings were not likely biased in any systematic way (Fig. 3C).

Informed by the results from the model simulations, we interpret the three dominant isotopic cycles that we observed to reflect differences in water use that fall along a spectrum between exclusive reliance on winter or summer precipitation. A timeseries analysis of these three water use patterns back to 1980, shows evidence for systematic low frequency shifts in seasonal water use preference or *plasticity* (Fig. 10). From the late 1980s to mid 1990s, 2000 to 2005 and post 2012, 80% of the rings were associated with dominant reliance on winter precipitation. On the other hand, there were brief periods surrounding 1985 and 2010, when preferential reliance on summer precipitation accounted for more than half of the growth rings. The temporal changes in seasonal water use by the trees closely followed changes in snowpack but in a counterintuitive way. Following multiple years of low snowpack, the trees increased their relative reliance on winter precipitation whereas during periods of increased snowpack, the relative use of summer rain increased (Fig. 10a). We note also that changes in snowpack and tree water use follow variations in tree ring width, such that periods of low snowpack and reliance on winter precipitation were associated with reduced aboveground growth (Fig. 10b). The correlation observed between tree ring widths and snowpack has been previously noted and has been interpreted to reflect the impact of reduced snowmelt on moisture stress (Woodhouse, 2003).

4 Discussion

The results presented here provide a first depiction of decadal variability in the seasonal origins of water used by two common conifers in Colorado using a proxy-based approach. It

is known that acquisition of soil water by plants involves diverse strategies that include dimorphic root systems (Dawson & Pate, 1996), preference for bound waters (moisture held at high matric potential) (Brooks et al., 2010), lateral and vertical scavenging (Grossiord et al., 2017) and hydraulic redistribution (Burgess, Adams, Turner, & Ong, 1998). Until now, limited datasets existed to test how the seasonal origins of plant water varied over timescales longer than 1-2 growing seasons, which hindered the ability to predict the response of ecosystem productivity, watershed hydrology or soil biogeochemical cycles to long and short term climate forcing (Eissenstat, Wells, Yanai, & Whitbeck, 2000; Joslin, Wolfe, & Hanson, 2000). The approach takes advantage of the fact that reliance on snowmelt through the growing season would lead to reduced variance in the isotopic ratio of the plant's water source and isotopic cycles in cellulose that would be driven primarily from surface climate and physiological forcing (Barbour et al., 2004; Gessler et al., 2009; Roden et al., 2000; Szejner et al., 2016). Alternatively, utilization of growing season precipitation would lead to isotopic cycles in the cellulose that reflect both an isotopically dynamic source water and changes in surface climate (Belmecheri et al., 2018; Treydte et al., 2014).

The field observations and tree-ring cellulose data from 2016 both suggest a transition from use of winter to summer precipitation midway through the growing season that likely reflected the response to reduced water content at depth along with moistening of surface soil during the onset of summer rains (Figs. 4 and S8). This behavior could be interpreted either as an illustration of the trees shifting from a deeper to shallower water source as the surface soil was moistened and the deeper soil dried (Dawson & Pate, 1996; Grossiord et al., 2017; White, 1989). The change in the isotopic ratio of the source water could also reflect penetration of summer rains to depth along preferential flow paths (Thomas et al., 2013). Our soil moisture measurements did not detect preferential flow of summer rains at depth but the sampling strategy was also not optimized to capture this phenomenon. The cellulose data, however, showed that the nearly equal use of summer and winter precipitation during 2016 was rather uncommon in the context of the last 37 years (22% of measured years), highlighting the presence of plastic behavior and the limitations of using one or two field seasons of xylem and soil water data to infer the seasonal origin of water used by trees.

The longer timeseries generated here indicated it was more common for the trees to preferentially rely on precipitation from either summer or winter sources rather than switching between the two during a growing season. One implication of this finding is that during years when snowmelt was the dominant water source, summer rain only minimally contributed to transpiration and was either evaporated or contributed to recharge and streamflow. Alternatively, during years of reliance on summer rain, snowmelt was only minimally transpired. We interpret this behavior to illustrate that trees are generally predisposed to preferential use of summer or winter precipitation as opposed to displaying higher frequency responses to evolving seasonal soil moisture conditions. It is important to note that preferential use of summer or winter precipitation was not simply a reflection of more or less snowmelt flooding the system as increased use of snowmelt actually occurred during periods of reduced snowfall. The inverse relationship between plant use of snowmelt and winter snowfall amount suggests the seasonal origins of water use is determined by interactions between vadose zone hydrology and root systems, rather than being controlled solely by the relative contributions of seasonal water to the watershed.

One possible way to interpret the observed variability in water use documented here is that it reflects changes in the soil depth that trees draw water from. If we presume the fine root distribution shifts over time in response to variations in the water table depth (Fan et al., 2017), this could set the condition for preferential reliance on deeper soil moisture (i.e. snowmelt) or shallower soil moisture (summer precipitation) (Drewniak, 2019; Iversen, 2010). The multi-year turnover time of fine roots (Matamala et al., 2003) could thus generate annual to inter-annual persistence in the depth that water is drawn from, which may explain why the seasonal origin of tree water use reconstructed here appears to retain a legacy for multiple years (Fig. 10). This explanation could be summarized by the following sequence: (1) the water table depth and deep soil moisture content change in response to the previous years' snowpack (Amenu et al., 2005), (2) as the water table drops, the trees respond by deepening their root systems,

which has the effect of increasing reliance on deeper waters (i.e. snowmelt) and (3) after multiple years of high snowpack and recharge, the water table rises and investment in shallow fine roots increases, which leads to increased reliance on near-surface soil moisture. A longer dataset of water table depths and root profiles along with more precise information on canopy conditions would be needed to test this hypothesis.

However, changes in seasonal origins of plant water do not necessarily imply that trees are changing the depth they are drawing water from. Rather, the changes in the seasonal origins of the water could be a reflection of changes in the downward mobility of summer precipitation through the root zone or upward mobility of snowmelt from deeper soil layers into the root zone (Kumar et al., 2019). During periods of increased snowfall, anomalously wet soil conditions can persist at depth for multiple years. The higher soil moisture content at depth has the effect of reducing the downward transport of surface soil moisture during the growing season and, consequently, summer precipitation remains in the root zone longer (Ghannam et al., 2016). In contrast, during periods of low snowpack when the soil moisture at depth is reduced, the summer rain moves downward rapidly which, in turn, dries out the surface soils and leads to reduced transpiration. As shown in Figure 10, periods of reduced snowpack and increased reliance on snowpack were also periods of low tree growth and thus decreased transpiration. If antecedent snowpack affects the residence time of summer rain in the root zone, it seems likely that snowmelt provides a baseline water source for the trees and during wetter periods when total transpiration increases, summer rain remains in the root zone longer and supports the increased water demand. During some years, the summer rain contribution begins early in the growing season and gives rise to the cellulose patterns in Cluster 2 whereas in other years the use of summer rain does not begin until later in the growing season as we observed during the 2016 field season (Fig. 7).

It also may be the case that changes in both the root profiles and hysteresis of deep soil moisture may explain the apparent multi-annual persistence of the seasonal water use preference. These two mechanisms, the former biotic and the latter abiotic, are not mutually exclusive and may feedback to each other giving rise to the large shifts between 30% to 80% reliance on winter precipitation over the last 4 decades (Fig. 10). There are also other plausible mechanisms that may be relevant such as the effect of reduced snowpack on the exposure of surface roots to frost damage. This could inhibit use of shallow waters (i.e. summer precipitation) for multiple years following low snowpack conditions (Inouye, 2008; Song, Zhu, Li, Zhang, & Li, 2018). However, the timeseries of frost exposure we derived from nearby meteorological data do not suggest this was a critical process in determining temporal changes in plant water use (Fig. S12). Alternatively, competition for surface waters between conifers and co-located deciduous trees (i.e. *P. tremuloides*) (Anderegg et al., 2013) and herbaceous species (Nippert & Knapp, 2007) could shift over time and drive variations in access to summer precipitation (West, Hultine, Jackson, & Ehleringer, 2007; Williams & Ehleringer, 2000). Stable isotopic measurements of xylem and soil water from a meadow nearby the Gothic site showed that two dominant forb species, *Helianthella quinquenervis* and *Erigeron speciosus* drew water from deeper ($\geq$20 cm) and shallow soil horizons ($\leq$10 cm), respectively (S. Saleska, unpublished). Understory plant species thus compete for water pools at different depths though their impact on the transpiration budget of the forest canopy is presumably small relative to the mature trees. The co-located species may also influence hydraulic redistribution and increase the upward mobility of winter precipitation to the root zone.

Our interpretation of how these trees modified their water use relies on the assumption that changes in the shape of the seasonal cycle in cellulose reflect shifts in the source water. While this interpretation is supported by the model simulations, it is important to note that there remain key sources of uncertainty in the method that limit quantitative inferences on seasonal water use (Allen et al., 2019). We lacked long in situ meteorological records of humidity and radiation that would have enabled more accurate forcing to the cellulose and canopy models. Furthermore, flux records of evapotranspiration or CO_2 and thermal imaging of the canopy would have allowed us to optimize the canopy model, SCOPE. Both of these datasets would have provided better constraints on how surface-atmosphere exchange influences the cellulose, which would have yielded better constraints on our estimates of trees' source water. In addition, the

canopy model lacked key ecosystem dynamics including the effect of changing soil moisture on stomatal conductance. The absence of this particular process may have led the model to miss changes in canopy exchange and temperature during sub-seasonal droughts. This could have led to an underestimation of the effect of VPD on the season cycle of cellulose. Additionally, the absence of a soil moisture-stomatal conductance feedback may have artificially extended the growing season during dry years. Indeed, we see that growing season length between years was likely artificially stable in the simulations (Fig. S13). Lastly, the cellulose model presumed that after carbon was fixed, it was immediately converted to cellulose. In reality, there are short lags (~week timescale) associated with translocating these sugars to the trunk and long lags if the tree utilized a prior year's carbohydrate pool for cellulose metabolism (Gessler et al., 2014). We did not include these processes because we lacked data to place a reasonable constraint on the necessary timescales. Failing to account for these lag processes likely means there is an offset in the seasonal timing of the cellulose timestamps and there may be some interannual carry-over effects in the observations that were not accounted for in the modeling. This issue becomes important if one is attempting to use cellulose data to precisely distinguish when in the growing season a transition between water sources actually occurred. Future work that will include measurements of the rate of biomass accumulation in cells layers (Cuny et al., 2015) and timeseries' of the isotopic ratio of leaf and trunk sugars, would be necessary to place quantitative timestamps on cellulose layers. Nevertheless, it is encouraging that the Monte Carlo simulations suggest that the three dominant cycles observed in the cellulose likely represent distinct water use scenarios (Fig. 9). We envision variants of this approach could be broadly applied in other watersheds where there is a strong seasonal cycle in the isotopic ratio of precipitation.

5 Conclusion

Abundant evidence shows that plants do not simply utilize the precipitation that recently fell but rather use legacy water reservoirs available from the multi-seasonal to multi-annual residence time of soil moisture. The use of this water from previous seasons, in turn, adds legacy to ecosystems by buffering the response of transpiration and primary productivity to current surface forcing. This study provides a proxy approach to study temporal dynamics of water use based on the seasonal cycle of the isotopic ratio of cellulose. Using a cluster analysis along with a mechanistic model for the isotopic ratio of cellulose, we were able to distinguish three broad classes of water use defined as: (1) exclusive reliance on winter precipitation, (2) summer precipitation, or (3) a mid season transition between water sources. The results indicate that over the last 4 decades, the forests exhibited a high degree of water use plasticity but also multi-annual persistence. Our observations suggest that once a preference for a seasonal water use was established, it remained for multiple years providing evidence for legacy effects in plant water use. These variations in water use were driven by changes in winter snowpack such that periods of highest snowpack were associated with a reduction in the relative reliance on this water source. One interpretation of this behavior is that during high snowpack periods there was increased tree growth and summer rain supported the increased water demands. Possible mechanisms to explain this may include high recharge from snow led to soil moisture anomalies at depth that increased the residence time of summer rain in the root zone. However, other mechanism(s) linking snowpack to water use may also be relevant including changes in the root profile or changing competition with co-existing species. Future work could use information on water use from cellulose isotope measurements to test processes in land surface models that are difficult to constrain such as dynamic roots (Drewniak, 2019), interactions between groundwater and soil moisture (Maxwell & Condon, 2016) or species competition. The results presented here nonetheless provide important new insights for watershed models and interpretations of isotope hydrographs. Specifically, depending on the multi-annual context of when an analysis is conducted, summer precipitation may be selectively routed through a watershed or utilized by plants. Lastly, this approach has the capacity to provide a broad spatial and temporal picture of how plants influence streamflow and recharge because it can be applied in other watersheds where instrumental observational are limited.

6 Captions

Figure 1: Topographic map showing the primary locations discussed in the manuscript and the approximate location and size of the grid cell associated with the North American Regional Reanalysis data used as inputs to canopy model (SCOPE) and cellulose model.

Figure 2: A high-resolution scan from one of the tree cores used for the isotopic analyses along with a typical annual cycle in the isotopic ratio of cellulose. The x-axis is defined here as the fractional position relative to the total length of the individual growth ring.

Figure 3: (A) The average annual cycle in cellulose anomalies broken up by site (ZR referring to Ziegler Reservoir) and species. The error bars capture one standard deviation around the mean. (B) The distribution of δ^{18}O for each site and species. (C) The distribution of δ^{18}O as aggregated from the modeling exercise described in Section 2.4.

Figure 4: (A) The stable oxygen isotopic ratios of various surface reservoirs during the 2016 growing season from Gothic, CO. Data presented with lines and uncertainty clouds are averages from multiple years of data with one standard deviation of uncertainty. The isotopic ratio of snowpack is derived from an integrated snowpack sample taken on April 1 and so represents only a single moment in time but was extended through the timeseries for comparison with the other pools. The isotopic ratio of the xylem water is shown as the average of all samples taken within that period of time. (B) Stable oxygen isotope ratio of soil and groundwater as a function of depth and time. The black dots represent the depth and time of soil water measurements while the blue and brown dots show the timing of precipitation (0 cm) and well-water measurements (3 m), respectively. A kriging method was used to interpolate the point measurements to provide the stable oxygen isotope surfaces (in color). The locations associated with the measurements are shown in Fig. 1 and data sources are listed in Tables S2 and S3.

Figure 5: (A) Three water use models shown as the relative fraction of snowmelt in the xylem stream. The green line and bar captures the specific mixture of snowmelt and summer rain used by the trees during the 2016 growing season based on a two end member mixing model. (B) The stable isotopic ratio of xylem water that emerged from each of the three models of seasonal water use patterns shown in Panel A. The green dots (as shown in Figure 4) were used to generate the model for seasonal water use as represented by the green line.

Figure 6: Flow chart showing the model sub-components and data streams used as inputs to both the SCOPE and cellulose biogeochemical models. In sequence from left to right: data streams are input into SCOPE to solve for canopy-atmosphere exchange. The outputs from the SCOPE model are used along with information on the isotopic ratio of source water and water vapor, as inputs to a model to predict the isotopic ratio or cellulose (Roden et al., 2000). The model was run with three different possible water use scenarios, which are color-coded as blue (snowmelt), green (snowmelt to summer precipitation) and red (summer precipitation). We show the approximate shape of the isotopic cycles in cellulose that emerged from forcing the model with the three different water sources. The model inputs, parametrizations and associated data sources are listed in Tables S1-S4.

Figure 7: (A-C) Results from the k-means clustering analysis of all the observed cellulose cycles. Gray lines are the individual cycles that fell into that cluster, the solid colored lines show the mean of all cycles and the dotted lines show the 25^{th} and 75^{th} percentiles around the mean. (D) The frequency of the three clusters shown in Panels A-C. (E-G) Results from the model simulations using the three difference water use patterns. The colors correspond directly to the colors used in Figure 6. The solid lines here show the mean of the 37 annual cycles and the gray bar shows the 25^{th} and 75^{th} percentiles around the mean.

Figure 8: (A) Cumulative annual growth measured from dendrometer bands (colored lines) and photosynthesis from the SCOPE model (Methods). The growth measurements were made monthly (as indicated by the points) from 2004-2010. The average and best-fit regression line over this period is shown. For photosynthesis, the model was run from 1980-2016 and the average over that period is shown. The dots mark 7 evenly-spaced increments (in terms of carbon fixation), which represents how the seasonal cellulose measurements were incremented. The uncertainty bars show the range of possible days when each increment was reached over the 37-year simulation. (B) The lag in days between when cumulative volume and carbon fix-

ation reach progressive increments as indicated by the gray area between curves in panel A. Growth and carbon fixation begin and end near the same time of the year but volumetric growth occurs more rapidly early in the season whereas carbon fixation occurs later (Cuny et al., 2015).

Figure 9: (A-C) The range of seasonal cycles in $\delta^{18}O$ that emerge from the Monte Carlo simulations using the three difference water use patterns described in the text. The colors associated with the different water use correspond to those used in Figs. 6 and 7. The shading captures the relative density of data at a given place on the graph. (D-F) Same as for A-C but the y-axes are now anomalies relative to each year. Note the difference in the range of isotopic variability (y-axes) between A-C and D-F.

Figure 10: (A) Timeseries showing the proportion of annual isotopic cycles that fell within Cluster 1, which is the pattern that emerged from reliance on snowmelt (colored wedges). This is plotted alongside the timeseries of snowfall for the previous three winters. (B) Timeseries of tree-ring widths averaged for all conifers from the two stands. Gray bars denote one standard deviation around the mean for each year.

Acknowledgments

The authors would like to thank Wendy Brown for collecting Copper Creek and groundwater samples for isotopic analysis as well as the entire staff of the Rocky Mountain Biological lab including billy barr for field support and providing weather data. The authors would like to thank Peter Brown from the Rocky Mountain Tree Ring Lab, Steve Nash from the Denver Museum of Nature and Science and Rebecca Brice from USGS and University of Arizona for field support in collecting the Snowmass tree ring samples. We thank Scott Saleska for providing the unpublished xylem water isotope data from the RMBL Research Meadow. We also acknowledge Jenny Bueno, Blanca Escutia and Ioana Stefanescu for their assistance in processing cellulose samples. The work was partially supported through NSF grant 1502776 to MB and the Johnson Family Memorial Fellowship Endowment to FR. MW was partially supported by DOE-DE-SC0014556. This material is partially based upon work supported through the Lawrence Berkeley National Laboratory's Watershed Function Scientific Focus Area. The U.S. Department of Energy (DOE), Office of Science, Office of Biological and Environmental Research funded the work under contract DE-AC02-05CH11231 (Lawrence Berkeley National Laboratory; operated by the University of California). The data associated with this study are archived and accessible from through the Rocky Mountain Biological Lab (http://www.rmbl.org/scientists/databases/) and through the DOE East River Watershed data portal (http://watershed.lbl.gov/data/).

References

Allen, S. T., Kirchner, J. W., Braun, S., Siegwolf, R. T., & Goldsmith, G. R. (2019). Seasonal origins of soil water used by trees. *Hydrology and Earth System Sciences*, *23*(2), 1199–1210.

Amenu, G. G., Kumar, P., & Liang, X.-Z. (2005). Interannual variability of deep-layer hydrologic memory and mechanisms of its influence on surface energy fluxes. *Journal of climate*, *18*(23), 5024–5045.

Anchukaitis, K. J., Evans, M. N., Lange, T., Smith, D. R., Leavitt, S. W., & Schrag, D. P. (2008). Consequences of a rapid cellulose extraction technique for oxygen isotope and radiocarbon analyses. *Analytical chemistry*, *80*(6), 2035–2041.

Anderegg, L. D., Anderegg, W. R., Abatzoglou, J., Hausladen, A. M., & Berry, J. A. (2013). Drought characteristics' role in widespread aspen forest mortality across colorado, usa. *Global Change Biology*, *19*(5), 1526–1537.

Anderson, L., Berkelhammer, M., & Mast, M. A. (2016). Isotopes in North American Rocky Mountain Snowpack 1993–2014. *Quaternary Science Reviews*, *131*, 262–273.

Barbour, M. M., Roden, J. S., Farquhar, G. D., & Ehleringer, J. R. (2004). Expressing leaf water and cellulose oxygen isotope ratios as enrichment above source water reveals evidence of a péclet effect. *Oecologia*, *138*(3), 426–435.

Belmecheri, S., Wright, W. E., Szejner, P., Morino, K. A., & Monson, R. K. (2018). Carbon and oxygen isotope fractionations in tree rings reveal interactions between cambial

phenology and seasonal climate. *Plant, cell & environment*.
Berkelhammer, M., Noone, D., Wong, T., Burns, S., Knowles, J., Kaushik, A., ... Williams, M. (2016). Convergent approaches to determine an ecosystem's transpiration fraction. *Global Biogeochemical Cycles*, *30*(6), 933–951.
Berkelhammer, M., & Stott, L. (2012). Secular temperature trends for the southern Rocky Mountains over the last five centuries. *Geophysical Research Letters*, *39*(17).
Berkelhammer, M., & Stott, L. D. (2009). Modeled and observed intra-ring δ 18 o cycles within late holocene bristlecone pine tree samples. *Chemical Geology*, *264*(1), 13–23.
Berry, Z. C., Evaristo, J., Moore, G., Poca, M., Steppe, K., Verrot, L., ... others (2018). The two water worlds hypothesis: Addressing multiple working hypotheses and proposing a way forward. *Ecohydrology*, *11*(3), e1843.
Bierkens, M. F., & Van den Hurk, B. J. (2007). Groundwater convergence as a possible mechanism for multi-year persistence in rainfall. *Geophysical Research Letters*, *34*(2).
Bowling, D. R., Schulze, E. S., & Hall, S. J. (2017). Revisiting streamside trees that do not use stream water: can the two water worlds hypothesis and snowpack isotopic effects explain a missing water source? *Ecohydrology*, *10*(1).
Bréda, N., Huc, R., Granier, A., & Dreyer, E. (2006). Temperate forest trees and stands under severe drought: a review of ecophysiological responses, adaptation processes and long-term consequences. *Annals of Forest Science*, *63*(6), 625–644.
Brooks, J. R., Barnard, H. R., Coulombe, R., & McDonnell, J. J. (2010). Ecohydrologic separation of water between trees and streams in a mediterranean climate. *Nature Geoscience*, *3*(2), 100–104.
Brown, P. M., Nash, S. E., & Kline, D. (2014). Identification and dendrochronology of wood found at the Ziegler Reservoir fossil site, Colorado, USA. *Quaternary Research*, *82*(3), 575–579.
Buenning, N. H., Stott, L., Yoshimura, K., & Berkelhammer, M. (2012). The cause of the seasonal variation in the oxygen isotopic composition of precipitation along the western us coast. *Journal of Geophysical Research: Atmospheres*, *117*(D18).
Bunde, A., Büntgen, U., Ludescher, J., Luterbacher, J., & Von Storch, H. (2013). Is there memory in precipitation? *Nature climate change*, *3*(3), 174–175.
Burgess, S. S., Adams, M. A., Turner, N. C., & Ong, C. K. (1998). The redistribution of soil water by tree root systems. *Oecologia*, *115*(3), 306–311.
Burk, R., & Stuiver, M. (1981). Oxygen isotope ratios in trees reflect mean annual temperature and humidity. *Science*, *211*(4489), 1417–1419.
Chang, E., Wolf, A., Gerlein-Safdi, C., & Caylor, K. K. (2016). Improved removal of volatile organic compounds for laser-based spectroscopy of water isotopes. *Rapid Communications in Mass Spectrometry*, *30*(6), 784–790.
Cuny, H. E., Rathgeber, C. B., Frank, D., Fonti, P., Mäkinen, H., Prislan, P., ... others (2015). Woody biomass production lags stem-girth increase by over one month in coniferous forests. *Nature Plants*, *1*(11), 15160.
Dawson, T. E., & Pate, J. S. (1996). Seasonal water uptake and movement in root systems of Australian phraeatophytic plants of dimorphic root morphology: a stable isotope investigation. *Oecologia*, *107*(1), 13–20.
DeNiro, M. J., & Epstein, S. (1981). Isotopic composition of cellulose from aquatic organisms. *Geochimica et Cosmochimica Acta*, *45*(10), 1885–1894.
Drewniak, B. (2019). Simulating dynamic roots in the energy exascale earth system land model. *Journal of Advances in Modeling Earth Systems*, *11*(1), 338–359.
Dubbert, M., & Werner, C. (2019). Water fluxes mediated by vegetation: emerging isotopic insights at the soil and atmosphere interfaces. *New Phytologist*, *221*(4), 1754–1763.
Eissenstat, D., Wells, C., Yanai, R., & Whitbeck, J. (2000). Building roots in a changing environment: implications for root longevity. *The New Phytologist*, *147*(1), 33–42.
Esper, J., Schneider, L., Smerdon, J. E., Schöne, B. R., & Büntgen, U. (2015). Signals and memory in tree-ring width and density data. *Dendrochronologia*, *35*, 62–70.
Evans, M. (2007). Toward forward modeling for paleoclimatic proxy signal calibration: A case study with oxygen isotopic composition of tropical woods. *Geochemistry, Geo-*

physics, Geosystems, *8*(7).

Fan, Y., Miguez-Macho, G., Jobbágy, E. G., Jackson, R. B., & Otero-Casal, C. (2017). Hydrologic regulation of plant rooting depth. *Proceedings of the National Academy of Sciences*, 201712381.

Ferguson, I. M., Jefferson, J. L., Maxwell, R. M., & Kollet, S. J. (2016). Effects of root water uptake formulation on simulated water and energy budgets at local and basin scales. *Environmental Earth Sciences*, *75*(4), 1–15.

Franke, J., Frank, D., Raible, C. C., Esper, J., & Brönnimann, S. (2013). Spectral biases in tree-ring climate proxies. *Nature Climate Change*, *3*(4), 360–364.

Gessler, A., Brandes, E., Buchmann, N., Helle, G., Rennenberg, H., & Barnard, R. L. (2009). Tracing carbon and oxygen isotope signals from newly assimilated sugars in the leaves to the tree-ring archive. *Plant, Cell & Environment*, *32*(7), 780–795.

Gessler, A., Ferrio, J. P., Hommel, R., Treydte, K., Werner, R. A., & Monson, R. K. (2014). Stable isotopes in tree rings: towards a mechanistic understanding of isotope fractionation and mixing processes from the leaves to the wood. *Tree physiology*, *34*(8), 796–818.

Ghannam, K., Nakai, T., Paschalis, A., Oishi, C. A., Kotani, A., Igarashi, Y., ... Katul, G. G. (2016). Persistence and memory timescales in root-zone soil moisture dynamics. *Water Resources Research*, *52*(2), 1427–1445.

Goldsmith, G. R., Allen, S. T., Braun, S., Engbersen, N., González-Quijano, C. R., Kirchner, J. W., & Siegwolf, R. T. (2019). Spatial variation in throughfall, soil, and plant water isotopes in a temperate forest. *Ecohydrology*, *12*(2), e2059.

Grossiord, C., Sevanto, S., Dawson, T. E., Adams, H. D., Collins, A. D., Dickman, L. T., ... McDowell, N. G. (2017). Warming combined with more extreme precipitation regimes modifies the water sources used by trees. *New Phytologist*, *213*(2), 584–596.

Helliker, B. R., Song, X., Goulden, M. L., Clark, K., Bolstad, P., Munger, J. W., ... others (2018). Assessing the interplay between canopy energy balance and photosynthesis with cellulose δ 18 o: large-scale patterns and independent ground-truthing. *Oecologia*, *187*(4), 995–1007.

Hu, J., Moore, D. J., Burns, S. P., & Monson, R. K. (2010). Longer growing seasons lead to less carbon sequestration by a subalpine forest. *Global Change Biology*, *16*(2), 771–783.

Inouye, D. W. (2008). Effects of climate change on phenology, frost damage, and floral abundance of montane wildflowers. *Ecology*, *89*(2), 353–362.

Iversen, C. M. (2010). Digging deeper: fine-root responses to rising atmospheric CO_2 concentration in forested ecosystems. *New Phytologist*, *186*(2), 346–357.

Johnson, J., Hamann, L., Dettman, D., Kim-Hak, D., Leavitt, S., Monson, R., & Papuga, S. (2017). Performance of induction module cavity ring-down spectroscopy (IM-CRDS) for measuring δ18O and δ2H values of soil, stem, and leaf waters. *Rapid Communications in Mass Spectrometry*, *31*(6), 547–560.

Joiner, J., Yoshida, Y., Zhang, Y., Duveiller, G., Jung, M., Lyapustin, A., ... Tucker, C. (2018). Estimation of terrestrial global gross primary production (gpp) with satellite data-driven models and eddy covariance flux data. *Remote Sensing*, *10*(9), 1346.

Joslin, J., Wolfe, M., & Hanson, P. (2000). Effects of altered water regimes on forest root systems. *The New phytologist*, *147*(1), 117–129.

Kahmen, A., Sachse, D., Arndt, S. K., Tu, K. P., Farrington, H., Vitousek, P. M., & Dawson, T. E. (2011). Cellulose δ18o is an index of leaf-to-air vapor pressure difference (vpd) in tropical plants. *Proceedings of the National Academy of Sciences*, *108*(5), 1981–1986.

Keel, S. G., Joos, F., Spahni, R., Saurer, M., Weigt, R. B., & Klesse, S. (2016). Simulating oxygen isotope ratios in tree ring cellulose using a dynamic global vegetation model. *Biogeosciences*, *13*(13), 3869–3886. doi: 10.5194/bg-13-3869-2016

Kumar, S., Newman, M., Wang, Y., & Livneh, B. (2019). Potential reemergence of seasonal soil moisture anomalies in north america. *Journal of Climate*.

Liang, S., Zhao, X., Liu, S., Yuan, W., Cheng, X., Xiao, Z., ... others (2013). A long-term

global land surface satellite (glass) data-set for environmental studies. *International Journal of Digital Earth*, *6*(sup1), 5–33.

Marshall, J. D., & Monserud, R. A. (2006). Co-occurring species differ in tree-ring δ18o trends. *Tree physiology*, *26*(8), 1055–1066.

Martin, J., Looker, N., Hoylman, Z., Jencso, K., & Hu, J. (2018). Differential use of winter precipitation by upper and lower elevation douglas fir in the northern rockies. *Global change biology*, *24*(12), 5607–5621.

Matamala, R., Gonzalez-Meler, M. A., Jastrow, J. D., Norby, R. J., & Schlesinger, W. H. (2003). Impacts of fine root turnover on forest npp and soil c sequestration potential. *Science*, *302*(5649), 1385–1387.

Maxwell, R. M., & Condon, L. E. (2016). Connections between groundwater flow and transpiration partitioning. *Science*, *353*(6297), 377–380.

Maxwell, R. M., Condon, L. E., Danesh-Yazdi, M., & Bearup, L. A. (2019). Exploring source water mixing and transient residence time distributions of outflow and evapotranspiration with an integrated hydrologic model and Lagrangian particle tracking approach. *Ecohydrology*, *12*(1), e2042.

Maxwell, R. M., & Kollet, S. J. (2008). Interdependence of groundwater dynamics and land-energy feedbacks under climate change. *Nature Geoscience*, *1*(10), 665–669.

Mesinger, F., DiMego, G., Kalnay, E., Mitchell, K., Shafran, P. C., Ebisuzaki, W., ... others (2006). North American Regional Reanalysis. *Bulletin of the American Meteorological Society*, *87*(3), 343–360.

Monson, R. K., Szejner, P., Belmecheri, S., Morino, K. A., & Wright, W. E. (2018). Finding the seasons in tree ring stable isotope ratios. *American journal of botany*.

Mote, P. W., Li, S., Lettenmaier, D. P., Xiao, M., & Engel, R. (2018). Dramatic declines in snowpack in the western us. *npj Climate and Atmospheric Science*, *1*(1), 2.

Nardini, A., Casolo, V., Dal Borgo, A., Savi, T., Stenni, B., Bertoncin, P., ... McDowell, N. G. (2016). Rooting depth, water relations and non-structural carbohydrate dynamics in three woody angiosperms differentially affected by an extreme summer drought. *Plant, cell & environment*, *39*(3), 618–627.

Nippert, J. B., & Knapp, A. K. (2007). Linking water uptake with rooting patterns in grassland species. *Oecologia*, *153*(2), 261–272.

Ogée, J., Barbour, M. M., Wingate, L., Bert, D., Bosc, A., Stievenard, M., ... others (2009). A single-substrate model to interpret intra-annual stable isotope signals in tree-ring cellulose. *Plant, Cell & Environment*, *32*(8), 1071–1090.

Phillips, S. L., & Ehleringer, J. R. (1995). Limited uptake of summer precipitation by bigtooth maple (*Acer grandidentatum Nutt*) and Gambel's oak (*Quereus gambelii Nutt*). *Trees*, *9*(4), 214–219.

Rempe, D. M., & Dietrich, W. E. (2018). Direct observations of rock moisture, a hidden component of the hydrologic cycle. *Proceedings of the National Academy of Sciences*, *115*(11), 2664–2669.

Restaino, C. M., Peterson, D. L., & Littell, J. (2016). Increased water deficit decreases Douglas fir growth throughout western US forests. *Proceedings of the National Academy of Sciences*, *113*(34), 9557–9562.

Roden, J. S., Lin, G., & Ehleringer, J. R. (2000). A mechanistic model for interpretation of hydrogen and oxygen isotope ratios in tree-ring cellulose. *Geochimica et Cosmochimica Acta*, *64*(1), 21–35.

Romero-Saltos, H., Sternberg, L. d. S., Moreira, M. Z., & Nepstad, D. C. (2005). Rainfall exclusion in an eastern Amazonian forest alters soil water movement and depth of water uptake. *American Journal of Botany*, *92*(3), 443–455.

Rossi, S., Deslauriers, A., Griçar, J., Seo, J.-W., Rathgeber, C. B., Anfodillo, T., ... Jalkanen, R. (2008). Critical temperatures for xylogenesis in conifers of cold climates. *Global Ecology and Biogeography*, *17*(6), 696–707.

Sala, O. E., Gherardi, L. A., Reichmann, L., Jobbagy, E., & Peters, D. (2012). Legacies of precipitation fluctuations on primary production: theory and data synthesis. *Philosophical Transactions of the Royal Society B: Biological Sciences*, *367*(1606),

3135–3144.

Schubert, B. A., & Jahren, A. H. (2015). Seasonal temperature and precipitation recorded in the intra-annual oxygen isotope pattern of meteoric water and tree-ring cellulose. *Quaternary Science Reviews*, *125*, 1–14.

Simard, M., Pinto, N., Fisher, J. B., & Baccini, A. (2011). Mapping forest canopy height globally with spaceborne lidar. *Journal of Geophysical Research: Biogeosciences*, *116*(G4).

Song, L., Zhu, J., Li, M., Zhang, J., & Li, D. (2018). Water use strategies of natural pinus sylvestris var. mongolica trees of different ages in hulunbuir sandy land of inner mongolia, china, based on stable isotope analysis. *Trees*, *32*(4), 1001–1011.

Sprenger, M., Leistert, H., Gimbel, K., & Weiler, M. (2016). Illuminating hydrological processes at the soil-vegetation-atmosphere interface with water stable isotopes. *Reviews of Geophysics*, *54*(3), 674–704.

Sprenger, M., Llorens, P., Cayuela, C., Gallart, F., & Latron, J. (2019). Mechanisms of consistently disconnected soil water pools over (pore) space and time. *Hydrology and Earth System Sciences Discussions*, 1–18.

Szejner, P., Wright, W. E., Babst, F., Belmecheri, S., Trouet, V., Leavitt, S. W., ... Monson, R. K. (2016). Latitudinal gradients in tree ring stable carbon and oxygen isotopes reveal differential climate influences of the North American Monsoon System. *Journal of Geophysical Research: Biogeosciences*, *121*(7), 1978–1991.

Thomas, E. M., Lin, H., Duffy, C. J., Sullivan, P. L., Holmes, G. H., Brantley, S. L., & Jin, L. (2013). Spatiotemporal patterns of water stable isotope compositions at the shale hills critical zone observatory: Linkages to subsurface hydrologic processes. *Vadose Zone Journal*, *12*(4).

Treydte, K., Boda, S., Graf Pannatier, E., Fonti, P., Frank, D., Ullrich, B., ... others (2014). Seasonal transfer of oxygen isotopes from precipitation and soil to the tree ring: source water versus needle water enrichment. *New Phytologist*, *202*(3), 772–783.

van der Tol, C., Verhoef, W., Timmermans, J., Verhoef, A., & Su, Z. (2009). An integrated model of soil-canopy spectral radiances, photosynthesis, fluorescence, temperature and energy balance. *Biogeosciences*, *6*(12), 3109–3129.

van der Tol, C., Berry, J., Campbell, P., & Rascher, U. (2014). Models of fluorescence and photosynthesis for interpreting measurements of solar-induced chlorophyll fluorescence. *Journal of Geophysical Research: Biogeosciences*, *119*(12), 2312–2327.

Vendramini, P. F., & Sternberg, L. d. S. (2007). A faster plant stem-water extraction method. *Rapid Communications in Mass Spectrometry*, *21*(2), 164–168.

West, A., Hultine, K., Jackson, T., & Ehleringer, J. (2007). Differential summer water use by *Pinus edulis* and *Juniperus osteosperma* reflects contrasting hydraulic characteristics. *Tree Physiology*, *27*(12), 1711–1720.

White, J. (1989). Stable hydrogen isotope ratios in plants: a review of current theory and some potential applications. In *Stable isotopes in ecological research* (pp. 142–162). Springer.

Williams, D. G., & Ehleringer, J. R. (2000). Intra-and interspecific variation for summer precipitation use in Pinyon–Juniper woodlands. *Ecological Monographs*, *70*(4), 517–537.

Woodhouse, C. A. (2003). A 431-yr reconstruction of western Colorado snowpack from tree rings. *Journal of Climate*, *16*(10), 1551–1561.

Zhang, Z. Q., Evaristo, J., Li, Z., Si, B. C., & McDonnell, J. J. (2017). Tritium analysis shows apple trees may be transpiring water several decades old. *Hydrological Processes*, *31*(5), 1196–1201.

Figure 1.

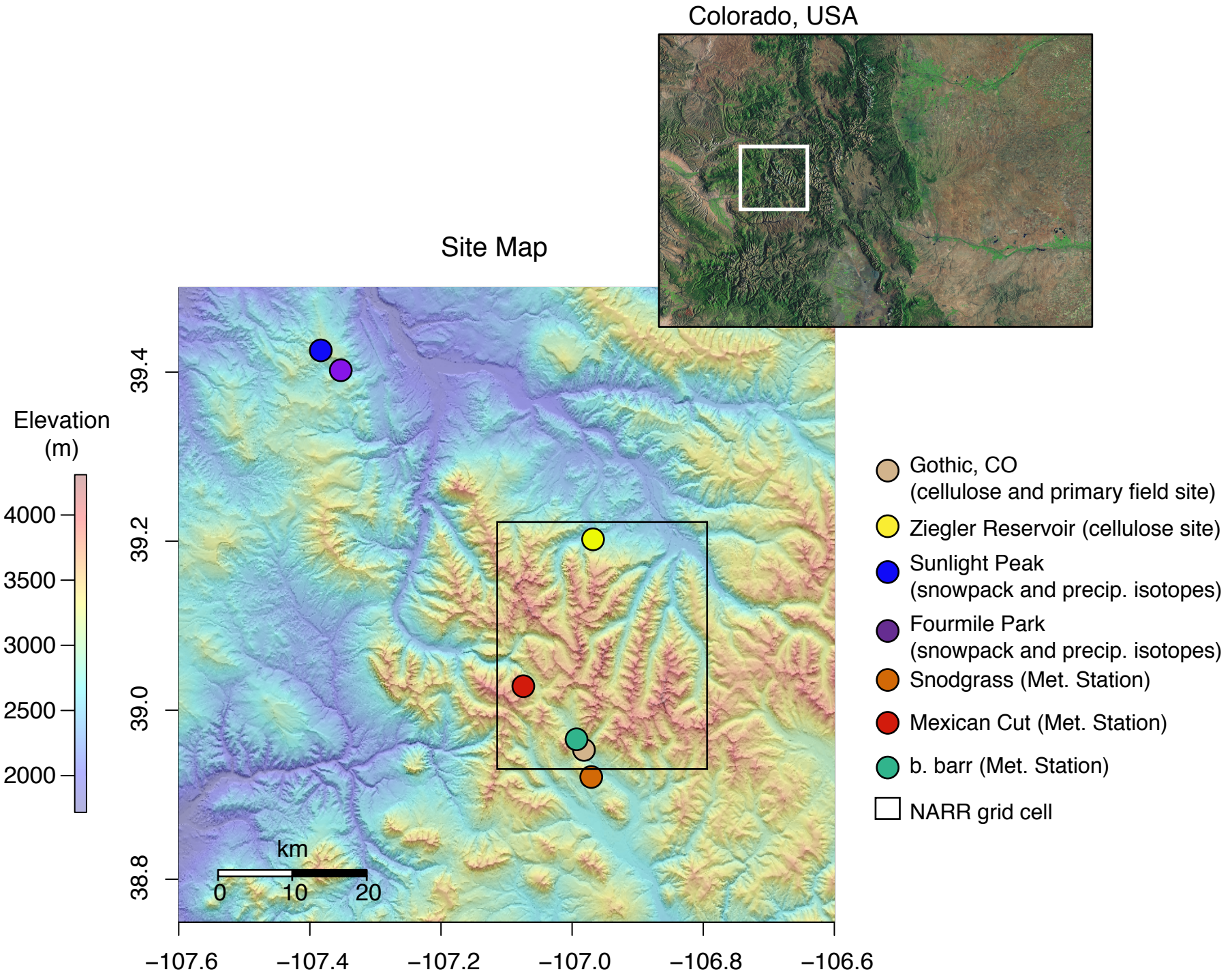
Colorado, USA
Site Map
Elevation
(m)
4000
3500
3000
2500
2000
39.4
39.2
39.0
38.8
km
0
10
20
−107.6
−107.4
−107.2
−107.0
−106.8
−106.6
Gothic, CO
(cellulose and primary field site)
Ziegler Reservoir (cellulose site)
Sunlight Peak
(snowpack and precip. isotopes)
Fourmile Park
(snowpack and precip. isotopes)
Snodgrass (Met. Station)
Mexican Cut (Met. Station)
b. barr (Met. Station)
NARR grid cell

Figure 2.

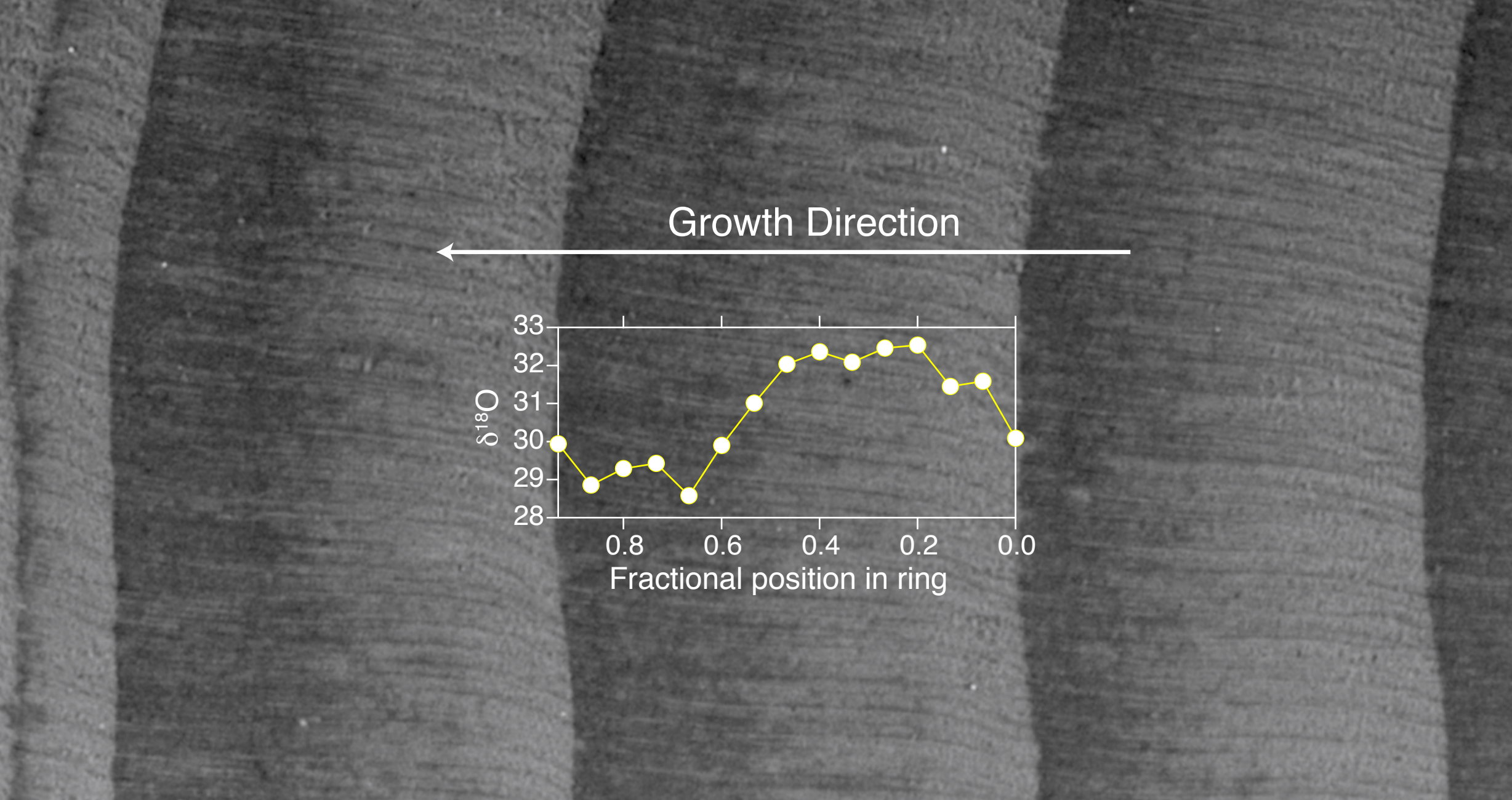
Growth Direction
33
32
31
30
29
28
δ18O
0.8
0.6
0.4
0.2
0.0
Fractional position in ring

Figure 3.

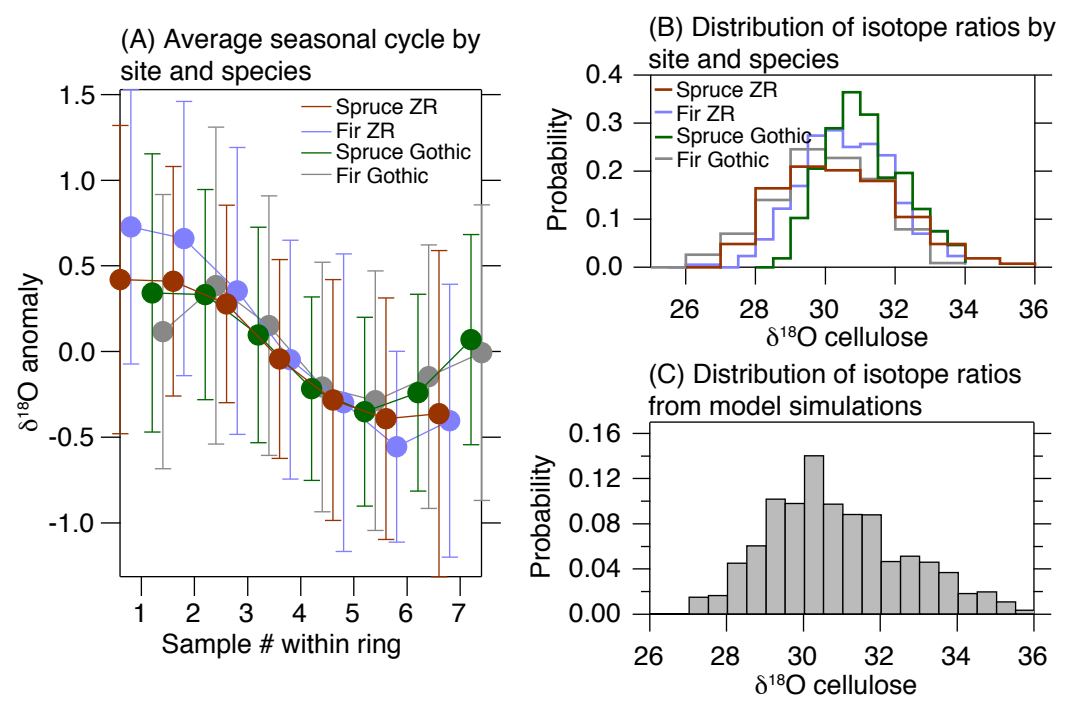
(A) Average seasonal cycle by site and species
Spruce ZR
Fir ZR
Spruce Gothic
Fir Gothic
δ18O anomaly
Sample # within ring
(B) Distribution of isotope ratios by site and species
Probability
δ18O cellulose
(C) Distribution of isotope ratios from model simulations
Probability
δ18O cellulose

Figure 4.

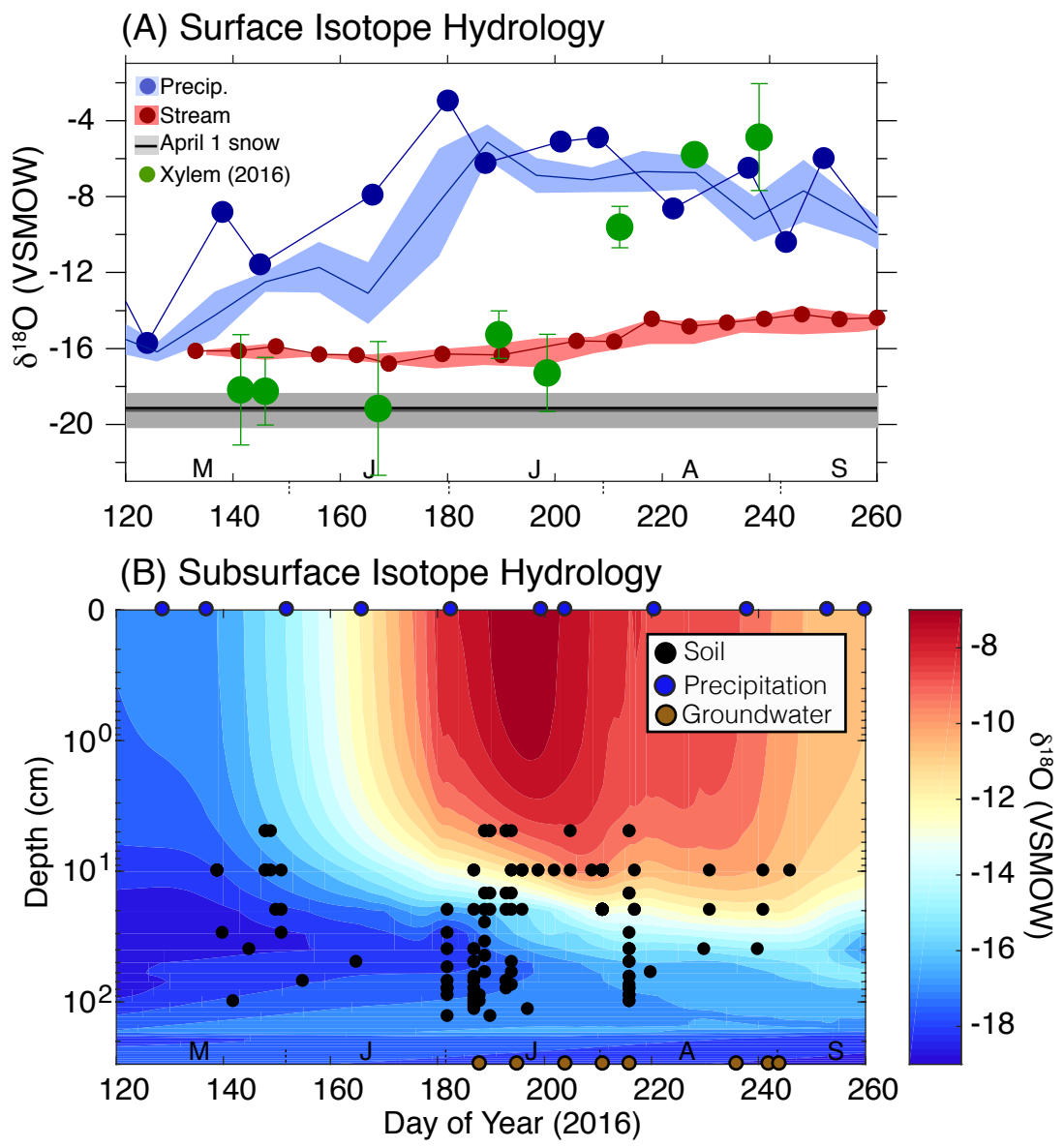
(A) Surface Isotope Hydrology
Precip.
Stream
April 1 snow
Xylem (2016)
δ18O (VSMOW)
-4
-8
-12
-16
-20
M
J
J
A
S
120
140
160
180
200
220
240
260
(B) Subsurface Isotope Hydrology
Soil
Precipitation
Groundwater
Depth (cm)
0
10^0
10^1
10^2
δ18O (VSMOW)
-8
-10
-12
-14
-16
-18
Day of Year (2016)

Figure 5.

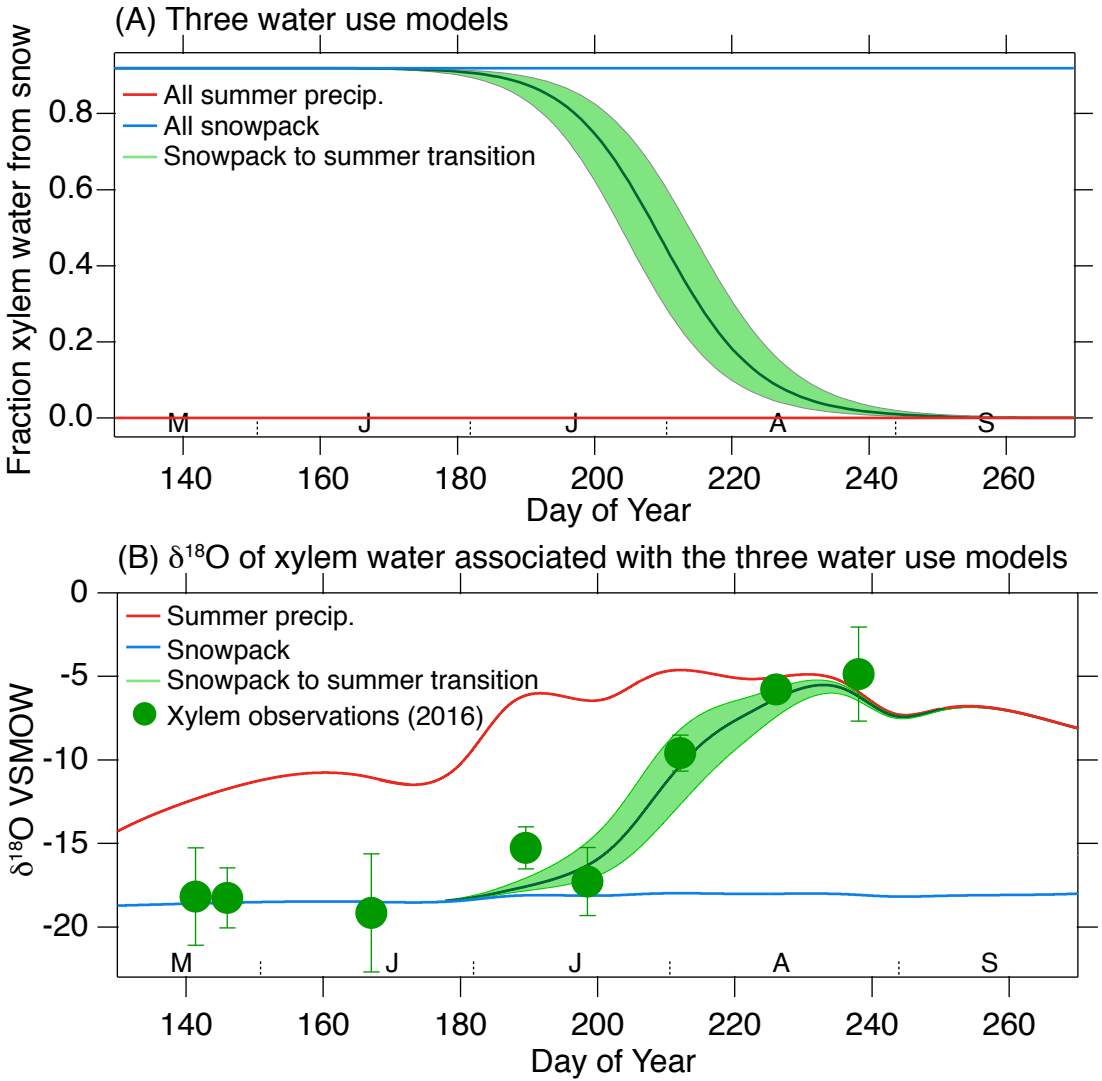
(A) Three water use models
Fraction xylem water from snow
All summer precip.
All snowpack
Snowpack to summer transition
0.0
0.2
0.4
0.6
0.8
M
J
J
A
S
140
160
180
200
220
240
260
Day of Year
(B) δ18O of xylem water associated with the three water use models
δ18O VSMOW
Summer precip.
Snowpack
Snowpack to summer transition
Xylem observations (2016)
0
-5
-10
-15
-20
M
J
J
A
S
140
160
180
200
220
240
260
Day of Year

Figure 6.

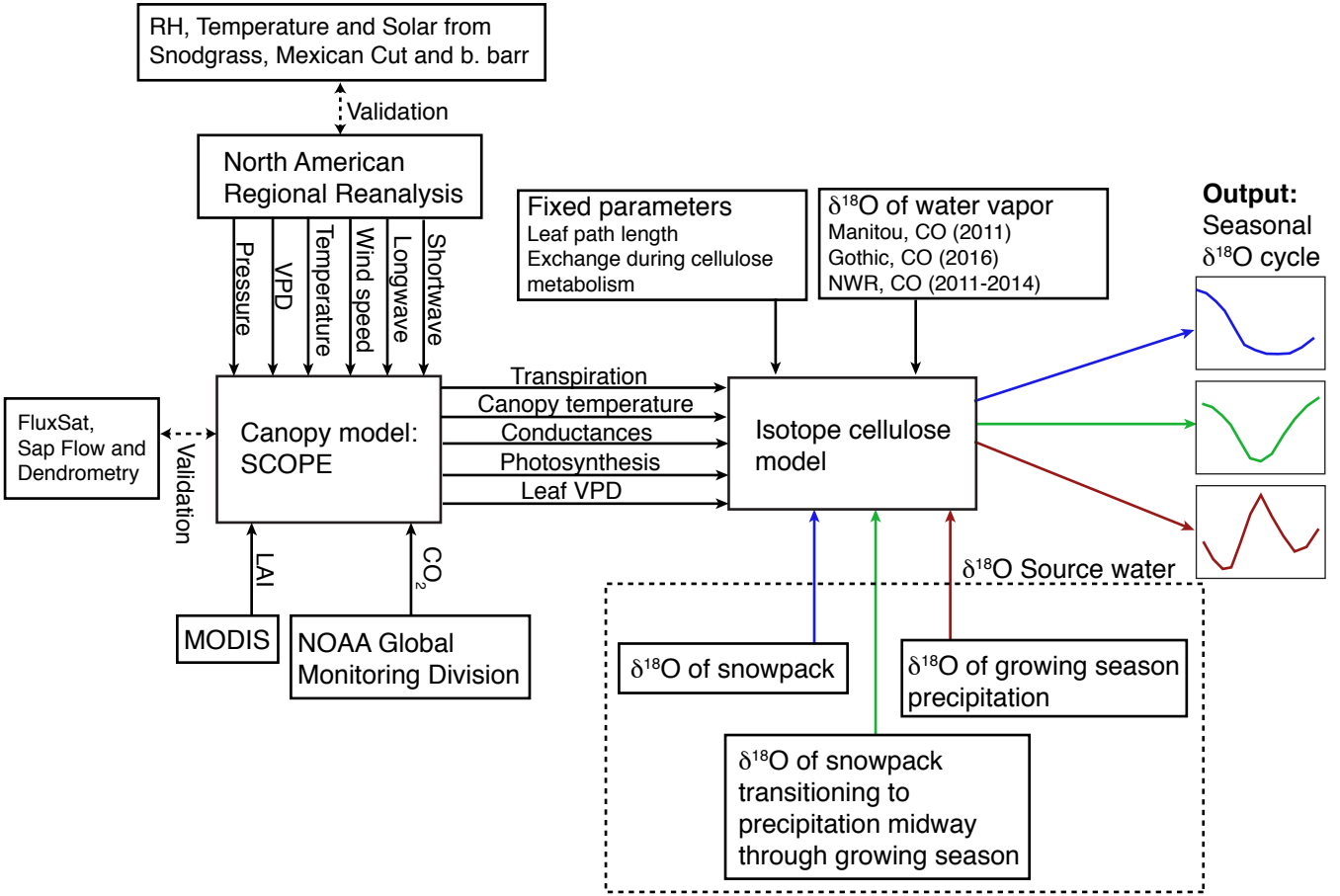
RH, Temperature and Solar from Snodgrass, Mexican Cut and b. barr
Validation
North American Regional Reanalysis
Pressure
VPD
Temperature
Wind speed
Longwave
Shortwave
Fixed parameters
Leaf path length
Exchange during cellulose metabolism
δ18O of water vapor
Manitou, CO (2011)
Gothic, CO (2016)
NWR, CO (2011-2014)
Output:
Seasonal
δ18O cycle
FluxSat,
Sap Flow and
Dendrometry
Validation
Canopy model:
SCOPE
Transpiration
Canopy temperature
Conductances
Photosynthesis
Leaf VPD
Isotope cellulose model
LAI
CO2
MODIS
NOAA Global Monitoring Division
δ18O Source water
δ18O of snowpack
δ18O of growing season precipitation
δ18O of snowpack transitioning to precipitation midway through growing season

Figure 7.

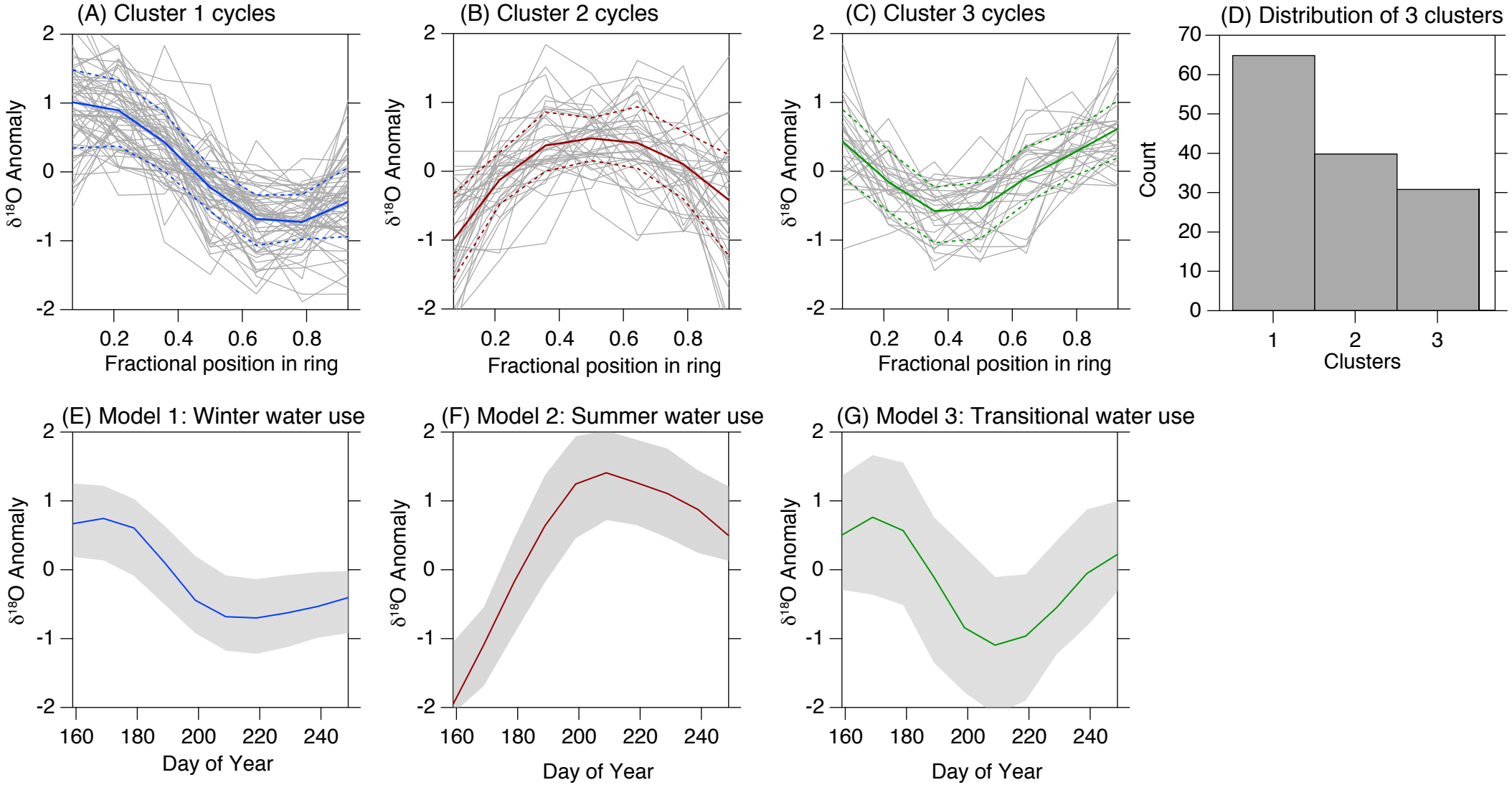
(A) Cluster 1 cycles
(B) Cluster 2 cycles
(C) Cluster 3 cycles
(D) Distribution of 3 clusters
δ18O Anomaly
Fractional position in ring
Count
Clusters
(E) Model 1: Winter water use
(F) Model 2: Summer water use
(G) Model 3: Transitional water use
Day of Year

Figure 8.

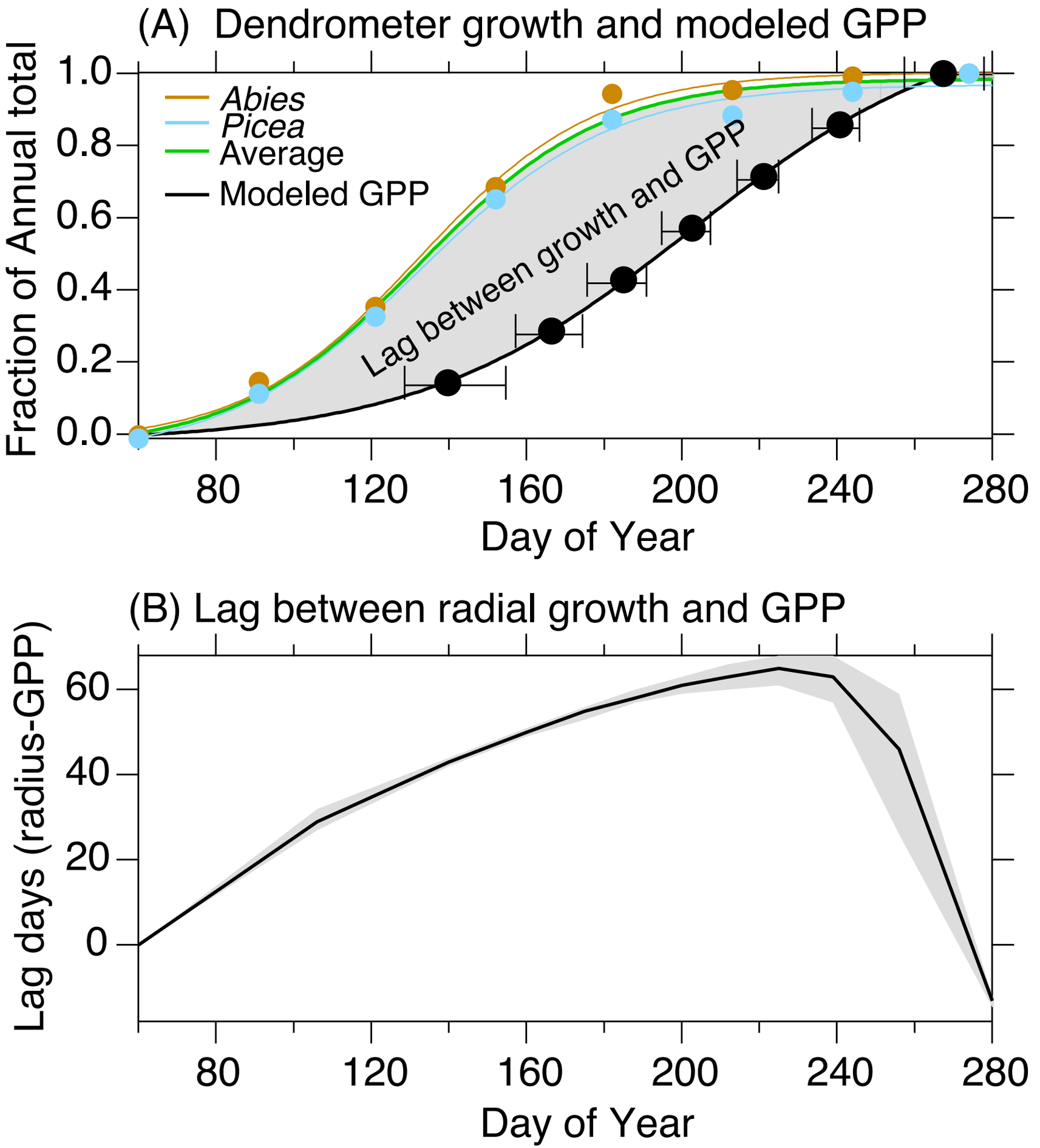
(A) Dendrometer growth and modeled GPP
Fraction of Annual total
1.0
0.8
0.6
0.4
0.2
0.0
Abies
Picea
Average
Modeled GPP
Lag between growth and GPP
80
120
160
200
240
280
Day of Year
(B) Lag between radial growth and GPP
Lag days (radius-GPP)
60
40
20
0
80
120
160
200
240
280
Day of Year

Figure 9.

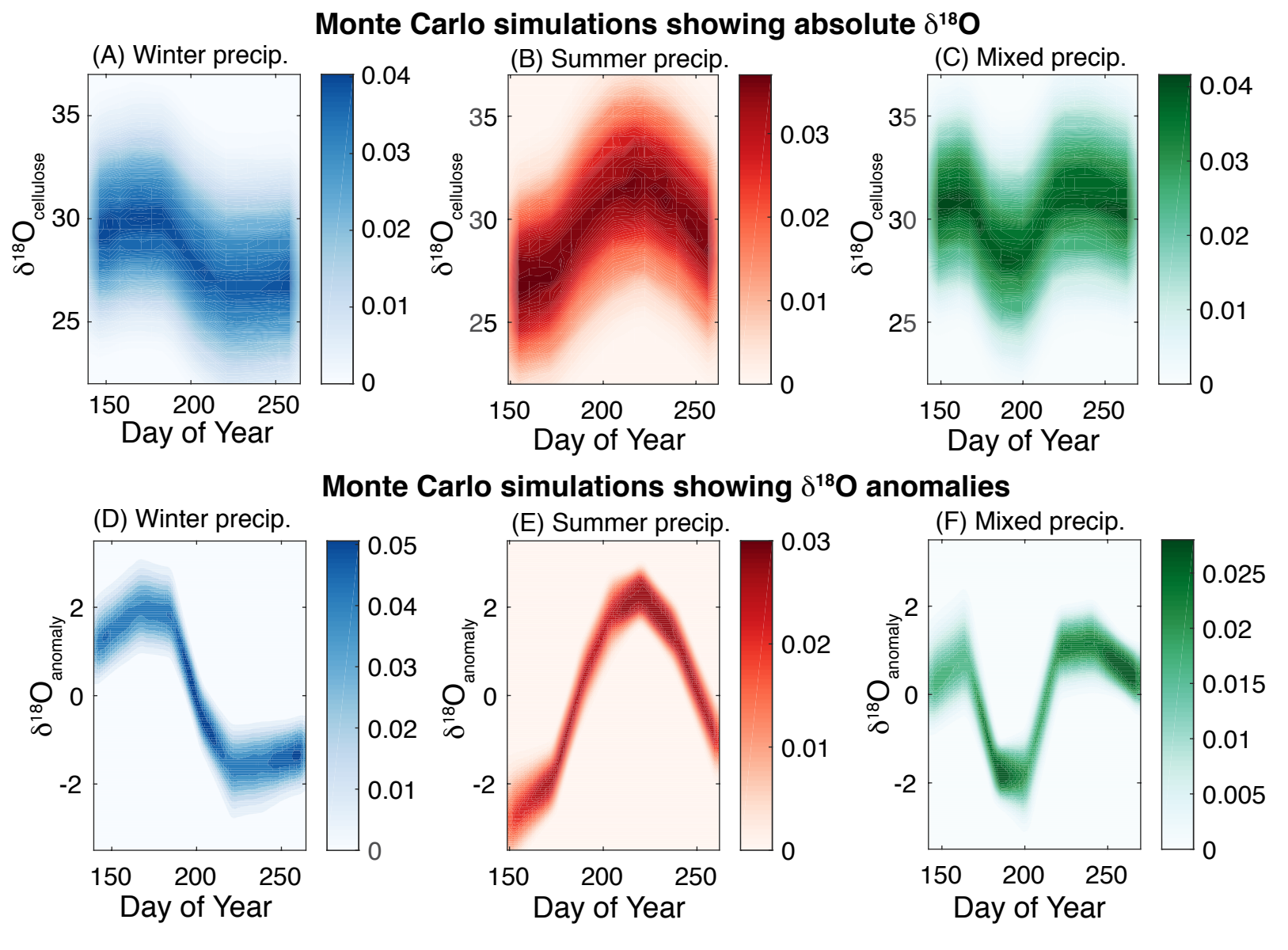
Monte Carlo simulations showing absolute δ18O
(A) Winter precip.
(B) Summer precip.
(C) Mixed precip.
δ18Ocellulose
Day of Year
Monte Carlo simulations showing δ18O anomalies
(D) Winter precip.
(E) Summer precip.
(F) Mixed precip.
δ18Oanomaly
Day of Year

Figure 10.

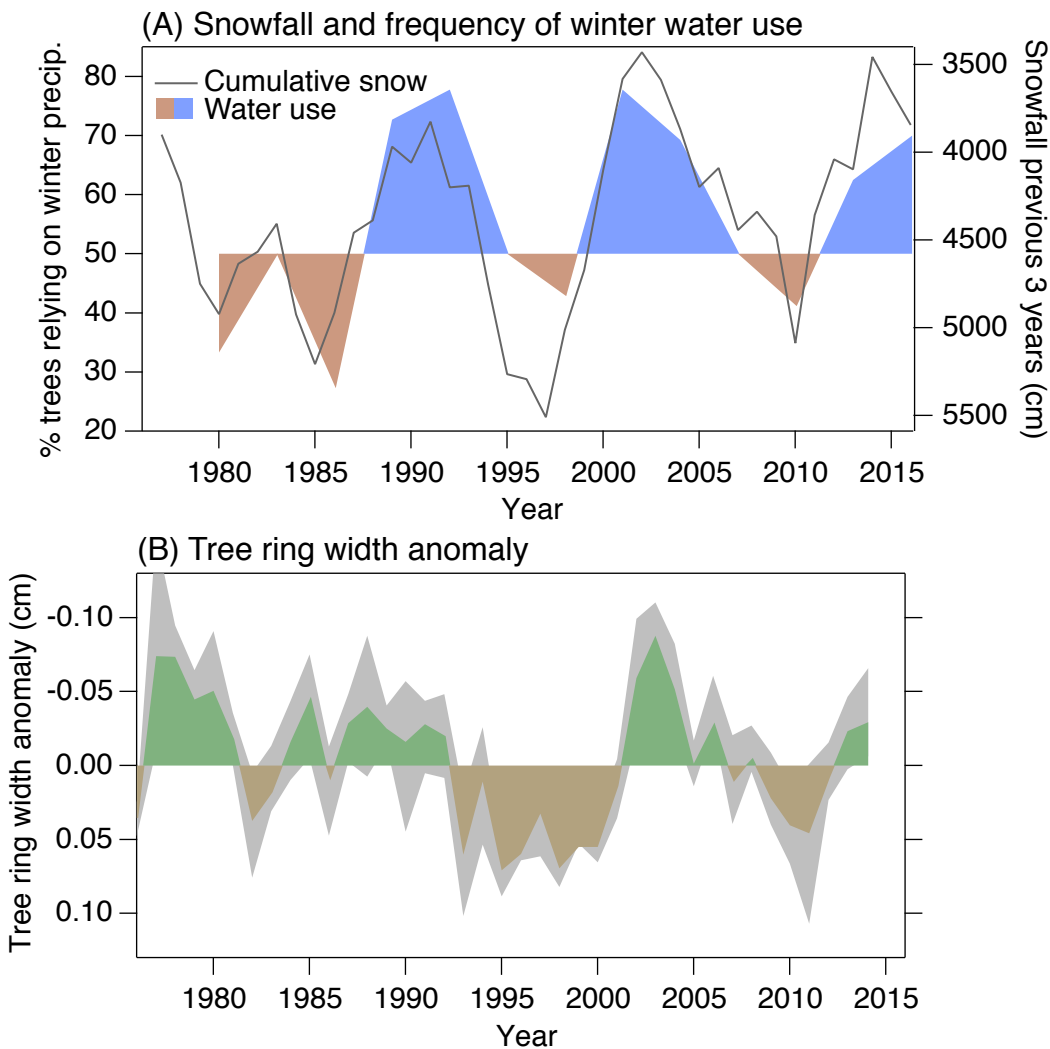
(A) Snowfall and frequency of winter water use
Cumulative snow
Water use
% trees relying on winter precip.
Snowfall previous 3 years (cm)
80
70
60
50
40
30
20
3500
4000
4500
5000
5500
1980
1985
1990
1995
2000
2005
2010
2015
Year
(B) Tree ring width anomaly
Tree ring width anomaly (cm)
-0.10
-0.05
0.00
0.05
0.10
1980
1985
1990
1995
2000
2005
2010
2015
Year